Title: The Rab GAP TBC1D4/AS160 interacts with the plasma membrane to positively regulate GLUT4 trafficking in adipocytes

Running Title: A positive role for AS160 in regulating GLUT4 trafficking

Authors: Shi-Xiong Tan[*1], Yvonne Ng[*1], James G. Burchfield[1], Jacqueline Stoeckli[1], David E. James[1,2,3]

[1] Diabetes and Obesity Research Program, The Garvan Institute of Medical Research, 384 Victoria St, Darlinghurst, Sydney, NSW 2010, Australia.
[2]School of Biotechnology and Biomolecular Sciences, University of New South Wales, Sydney, NSW 2050, Australia.
[3]Corresponding author d.james@garvan.org.au, Tel: +61-2-92958210;
*These authors contributed equally to this work
Fax:+61-2-92958201

Abstract

The RabGAP TBC1D4/AS160 regulates GLUT4 trafficking by binding to intracellular GLUT4 vesicle cargo like IRAP and inhibiting GTP Loading of Rabs that mediate GLUT4 translocation to the PM.. Akt-dependent phosphorylation of AS160 overcomes this inhibitory effect. Previously we identified a finite pool of AS160 at the PM in adipocytes that is highly phosphorylated in response to insulin (Ng et al., 2010). Here we show that AS160 associates with the PM through a PH-like domain at its N-terminus, distinct from the region that is important for its interaction with IRAP. This domain is highly conserved in the mammalian AS160 homolog, TBC1D1 and its counterpart in *Drosophila*, Pollux. PM localization of AS160 was mediated through interaction of positively charged residues in the PH-like domain and negatively charged lipids. Mutation of the two conserved lysine 215/216 residues abrogated lipid binding and PM targeting of AS160 but not IRAP binding. By studying the effects of AS160 mutants, that were either selectively impaired for IRAP or PM binding or constitutively targeted to the PM, by overexpressing them in adipocytes we were able to delineate two separate functions for AS160 in GLUT4 trafficking: an inhibitory function that mapped to the IRAP binding domain and a potentiating role mapping to the conserved lysines in the PH-like domain. The potentiating effect did not require the GAP function of AS160. This demonstrates that AS160 has both positive and negative roles in GLUT4 trafficking in adipocytes indicating that AS160 may play a crucial relay function in Rab GTP loading and fusion of GSVs with the PM.

Introduction

One of the major actions of insulin is to stimulate recruitment of the facilitative glucose transporter 4 (GLUT4) from intracellular vesicles to the plasma membrane (PM) to mediate glucose uptake into fat and muscle cells. The phosphatidylinositide 3-kinase (PI3K) and Akt/PKB signaling

pathway plays a fundamental role in this process (Whiteman et al., 2002). Akt mediates its myriad of functions via its ability to phosphorylate key targets that are intimately involved in the regulation of numerous fundamental cell biological processes such as increased glucose transport. In regard to the latter, the Akt substrate AS160/TBC1D4, has been shown to play a major role in insulin-regulated glucose transport by manipulating the translocation of GLUT4 to the PM (Eguez et al., 2005; Kane et al., 2002; Larance et al., 2005; Ramm et al., 2006; Sano et al., 2003; Stockli et al., 2008; Zeigerer et al., 2004). AS160 possesses a RabGAP/TBC domain at its C terminus flanked by a calmodulin binding domain and two phosphotyrosine-binding (PTB) domains at the N-terminus. PTB domains are commonly found in scaffolding proteins that often contain additional modular domains. Hence, such proteins often play a role in regulating the assembly of protein complexes (van der Geer and Pawson, 1995; Yan et al., 2002). There are over 50 members of the Rab GAP/TBC family yet few members possess PTB domains. Intriguingly, TBC1D1, a RabGAP that is homologous to AS160 and implicated in GLUT4 trafficking also has a similar domain structure at its N-terminus (Chen et al., 2008; Peck et al., 2009; Roach et al., 2007). Therefore, the presence of PTB domains in the N-terminus of these proteins likely encodes part of their unique function that is linked to GLUT4 translocation to the membrane.

AS160 was originally discovered as an insulin-regulated phosphoprotein in adipocytes (Kane et al., 2002; Sano et al., 2003; Zeigerer et al., 2004). Akt stimulates AS160 phosphorylation at Ser341 and Thr642 and this triggers 14-3-3 binding (Geraghty et al., 2007; Ramm et al., 2006). This plays a vital role in the regulation of GLUT4 trafficking since overexpression of an AS160 mutant, in which four of the phosphorylation sites were mutated to alanine (known as AS160-4P), inhibited insulin-stimulated GLUT4 insertion into the PM (Eguez et al., 2005; Ramm et al., 2006; Sano et al., 2003; Stockli et al., 2008; Zeigerer et al., 2004). Mutating the crucial arginine residue in the RabGAP domain overcame the inhibitory effect of AS160-4P (Miinea et al., 2005; Sano et al., 2003). These data provide a functional link between phosphorylation and the GAP activity of AS160 and suggest that AS160 GAP activity plays an essential role in GLUT4 trafficking to the PM. Overexpression of wild-type AS160 in adipocytes has no significant effect on basal or insulin-stimulated GLUT4 translocation to the PM, indicating that the level of AS160 is not rate-limiting (Sano et al., 2003; Zeigerer et al., 2004). Knock down of AS160 in adipocytes increased basal GLUT4 translocation (Brewer et al., 2011; Eguez et al., 2005) giving rise to the notion that AS160 plays a negative regulatory role in insulin-stimulated GLUT4 trafficking. Subsequently, it was shown that AS160 interacts with intracellular GLUT4 vesicles, in part via its association with the insulin-regulated aminopeptidase (IRAP), a co-inhabitant of these vesicles (Peck et al., 2006). This interaction was overcome by insulin either due to AS160 phosphorylation *per se* or concomitant 14-3-3 binding (Ramm et al., 2006).

These findings led to a model where AS160 binds to GSVs in the basal state to maintain its substrate Rab GTPase(s) in a GDP-loaded inactive form, thus retaining GSVs inside the cell. Upon insulin stimulation, Akt phosphorylates AS160 resulting in 14-3-3 binding and dissociation of AS160 from GSVs allowing GTP loading and activation of a Rab on GSVs that is required for GLUT4 trafficking to the PM (Geraghty et al., 2007; Kane et al., 2002; Larance et al., 2005; Ramm et al., 2006; Sano et al., 2003). This model denotes an inhibitory function for AS160 in GLUT4 trafficking. However, there are two potential caveats to this model. First, reduction of AS160 in adipocytes using shRNA results in two phenotypes: increased GLUT4 at the PM in the basal state and blunted insulin-stimulated translocation of GLUT4 to the PM (Brewer et al., 2011; Eguez et al., 2005). The former is consistent with the above model while this is not the case for the latter. Second, the release of AS160 from GSVs is not necessary for insulin-dependent translocation to the PM. This raises the possibility that AS160 may in fact remain associated with GSV cargo until after fusion with the PM (Koumanov et al., 2011; Stockli et al., 2008). Based on these observations we hypothesized that AS160 might fulfill sequential negative and positive regulatory roles in GLUT4 trafficking.

We have reported previously that there is a finite pool of AS160 at the PM in adipocytes that is highly phosphorylated in response to insulin implicating an important role for the GAP at this location (Ng et al., 2010). Here we show that a PH-like domain in the N-terminus of GLUT4 confers binding to negatively charged phospholipids and this binding domain is distinct from the IRAP binding domain. The association of AS160 with the PM mediates a potentiating effect on GLUT4 trafficking while its association with IRAP impedes GLUT4 trafficking. These data unveil a new function for AS160 whereby its GAP activity may be upstream of a scaffold function that plays a key role in docking/fusion of GLUT4 vesicles with the PM.

Results

AS160 is targeted to the PM via its N-terminus

To determine which domain mediates the interaction of AS160 with the PM, the relative PM localization of Flag-tagged AS160 truncation mutants was examined in HEK293E cells. The cationic silica method (Larance et al., 2005) was used to isolate PM and this method was robust as indicated by the enrichment of the PM marker Syntaxin4 (Fig. 1B). Consistent with our previous findings (Ng et al., 2010), full-length AS160 was enriched in the PM. $AS160_{1\text{-}924}$ but not $AS160_{719\text{-}1299}$ was enriched in the PM fraction to the same extent as full-length AS160 (Fig. 1C) indicating that the PM localization signal lies within the AS160 N-terminus. To determine the minimal region required for PM targeting of AS160 we constructed a series of additional N-terminal truncations. $AS160_{1\text{-}440}$ contains the two PTB domains; $AS160_{1\text{-}365}$ lacks the second PTB domain but retains the

spacer region prior to the second PTB domain; and $AS160_{1-190}$ retains the first PTB domain but lacks the spacer region (Fig. 1A). $AS160_{1-440}$ and $AS160_{1-365}$ both localized to the PM to a similar extent as full-length AS160 (Fig. 1D), indicating that the second PTB domain is dispensable for PM association.

Mapping the IRAP binding domain in AS160

Previously it has been reported that a similar domain within AS160 to that described above encodes the IRAP binding domain (Peck et al., 2006; Ramm et al., 2006). Thus, one possibility is that AS160 interacts with the PM *via* its interaction with IRAP. We used a similar strategy to that described above to determine the overlap between the IRAP and PM binding domains. First we mapped the minimal AS160 binding domain in the IRAP cytosolic domain to residues 1-58 (Fig. 1E) whereas mutation of lysine residues 53 and 54 to alanine in this IRAP fragment abolish this interaction (Fig. 1E). A GST-fusion protein comprising IRAP 1-58 was shown to interact with $AS160_{1-365}$ but not to $AS160_{365-1299}$ (Fig. 1F). These data indicate that the PM interaction domain lies within the same region of AS160 that interacts with IRAP.

Amino acid residues 190-365 of AS160 are required for PM localization

To further delineate the PM and IRAP binding domains in AS160 we set out to determine the critical region within the AS160 N-terminus required for its interaction with the PM. Given that a significant reduction in PM association was observed for $AS160_{1-190}$ (Fig. 1D) we postulated that the PM localization domain may lie between the two PTB domains encompassing residues 190-365. Consistent with this, $AS160_{190-365}$ was enriched in the PM to a greater extent than $AS160_{1-365}$ (Fig. 2A). Interestingly, when the domain including amino acid residues 190-365 were analyzed using the NCBI conserved domain platform (Marchler-Bauer et al., 2009) it was predicted to contain a partial pleckstrin-homology (PH)-like, core region between residues 190-239. To test this prediction we generated $AS160_{239-365}$ lacking the PH-like core domain and expressed this in HEK293E cells. This construct did not localize to the PM (Fig. 2A), indicating that residues 190-239 likely play a key role in PM targeting of AS160.

To further determine if the 190-239 region is important for PM localization of AS160, this domain was deleted from full-length AS160 (AS160-ΔPH) and its ability to localize to the PM was determined. AS160-ΔPH displayed reduced PM association compared to full-length AS160 (Fig. 2B) and this was further verified by subcellular fractionation (Supp. Fig. 1A). These data confirm the importance of the 190-239 region in mediating PM localization of AS160.

The closest homolog of AS160 in mammals is TBC1D1 and both genes are homologous to a *Drosophila melanogaster* gene known as Pollux (Bernards, 2003). The putative PM targeting signal

in AS160 (residues 190-239) is highly conserved in these TBC proteins (Supp. Fig. 2), indicating that this domain likely confers a similar function. Consistent with this, TBC1D1 and Pollux, but not two other TBC proteins, RabGAP1 and TBC1D13, displayed enhanced PM association similar to AS160 (Fig. 2C). Collectively, these data indicate that the 190-239 region of AS160 is involved in its targeting to the PM and that this function is conserved in TBC1D1 and Pollux.

To verify the PM targeting of AS160, we next developed a morphological assay based upon live-cell Total Internal Reflection Fluorescence Microscopy (TIRFM) imaging in 3T3-L1 adipocytes. This method resolves the presence of fluorescently tagged proteins at or just beneath the PM. We expressed EGFP tagged versions of several AS160 N-terminal mutants in 3T3-L1 adipocytes. Fluorescence intensity in the TIRF zone was normalized to total cellular fluorescence, measured via epifluorescence, to correct for differences in total expression. EGFP-AS160$_{190-365}$ localized to the TIRF zone to a greater extent compared to EGFP-AS160$_{239-365}$ and the EGFP-only controls (Figs. 2D & 2E). EGFP-AS160$_{190-239}$ was also enriched in the TIRF zone (Figs. 2D & 2E), albeit to a lesser extent as compared to EGFP-AS160$_{190-365}$, indicating that residues 190-239 are sufficient but not as effective in mediating PM localization of AS160 in 3T3-L1 adipocytes.

We next set out to determine if the PM localization region of AS160 could substitute for a known PM binding domain of a well-characterized protein. Activation of Akt requires its translocation to the PM and this is mediated via the interaction of a PH domain in Akt with PI(3,4,5)P3 in the PM. This interaction leads to phosphorylation of Akt at Thr308 and Ser473 (Alessi et al., 1996; Sarbassov et al., 2005). We substituted the PH domain of Akt1 with AS160$_{190-239}$, AS160$_{239-365}$, or AS160$_{190-365}$ and expressed these constructs in CHO-IR/IRS-1 cells. As a measure of PM targeting, we measured phosphorylation of these constructs at Thr308 and Ser473. In agreement with previous studies (Hausdorff et al., 1999; Kohn et al., 1996a), myristoylated ΔPHAkt1, which is constitutively targeted to the PM was robustly phosphorylated at both sites in the absence of insulin (Fig. 2F). The AS160$_{190-239}$ΔPHAkt1 and AS160$_{190-365}$ΔPHAkt1 both conferred strong Akt phosphorylation compared to AS160$_{239-365}$ΔPHAkt1 in the absence of insulin (Figs. 2F & 2G). Intriguingly, addition of growth factor was not required to achieve Akt phosphorylation for the Akt chimera suggesting that the 190-365 domain in AS160 may bind to PI(4,5)P2 which is constitutively present at the PM of most cells. Collectively, these data indicate that amino acids 190-365 in AS160 are sufficient to mediate PM localization of AS160 in a range of cell types.

AS160$_{190-365}$ binds to acidic phospholipids but not neutral lipids

In view of our observations that the AS160/Akt chimera targets constitutively to the PM, the crucial PM binding domain in AS160 comprises a potential PH-like domain and PH domains often

associate with phospholipids through electrostatic interactions (Kutateladze, 2010; Lemmon, 2008) we next wanted to test the hypothesis that AS160 interacts with the PM via an interaction with phospholipids. The partial PH-like, core domain in AS160 contains several positively charged amino acids (Supp. Fig 2), which may confer its interaction with negatively charged phospholipids. Residues K209, K215, K216, K228 and R236 of AS160 are highly conserved across species and are also found in Pollux and TBC1D1 (Supp. Fig 2). Mutation of two of these lysine residues at 215 and 216 was sufficient to impair PM targeting of $AS160_{190\text{-}365}$ (Fig. 3A). This observation was recapitulated in 3T3-L1 adipocytes using EGFP fusion constructs in live-cell TIRFM, where EGFP-$AS160_{190\text{-}365KK215/216AA}$ had reduced expression in the TIRF zone (Fig. 3B).

We next showed that the AS160 *N*-terminus binds directly to phospholipids *in vitro* (Fig. 3C). Significant binding of purified GST-$AS160_{190\text{-}365}$ to acidic phospholipids was observed, but binding to neutral lipids was not observed (Fig. 3C). An interaction was observed with most phosphorylated forms of PI but not with PI itself (Fig. 3C). Importantly, GST-$AS160_{190\text{-}365}$ bound strongly to PI(4,5)P2 and PI(3,4,5)P3, which are phospholipids that are highly abundant at the PM. The strong binding of this domain to PI(4,5)P2 is in agreement with the *in vivo* observation (Figs. 2F & 2G). Consistent with its weak association with the PM using biochemical and morphological approaches (Figs. 2A, 2E to 2G), GST-$AS160_{239\text{-}365}$ did not bind to any phospholipids (Fig. 3C). GST-$AS160_{190\text{-}365}$ KK215/216AA lost the ability to bind to phospholipids (Fig. 3C) consistent with these residues forming a key part of the lipid binding domain. The observation that full-length AS160 KK215/216AA displayed reduced localization to the PM provided further confirmation that lipid binding is a major mechanism for the interaction of AS160 with the PM (Fig. 3D).

AS160 associates with IRAP and the PM via distinct mechanisms.

The IRAP interaction domain in AS160 is located between residues 1-365 of AS160 and this includes the PM interaction domain (Figs. 1 & 2). We next wanted to determine the relationship between these interactions. The same set of AS160 mutants as described above were used in an IRAP binding assay. $AS160_{365\text{-}1299}$ displayed minimal interaction with $IRAP_{1\text{-}58}$, whereas AS160KK retained a significant interaction with IRAP (Figs. 4A & 4B). These data indicate that AS160 interacts with lipids and IRAP *via* distinct mechanisms.

In view of the conservation in the PM binding domain in Pollux (Supp. Fig. 2) we next wanted to examine if Pollux also contained the IRAP binding domain. We reasoned that if the PM interaction domain in AS160 is sufficient for its interaction with IRAP then Pollux should interact with IRAP to the same extent as AS160. The data from the GST-$IRAP_{1\text{-}58}$ pull down indicated that Pollux only bound to IRAP with < 50% the efficiency of that observed with AS160 (Fig. 4C). We then constructed a Pollux-AS160 chimera whereby the PM localization domain of AS160 (amino

acids 1-365) was replaced with the corresponding region from Pollux (amino acids 1-334). This Pollux-AS160 chimera retained its binding to the PM (Fig. 4D) but not to IRAP (Fig. 4E). Collectively, these data indicate that AS160 interacts with the PM and IRAP *via* discrete binding modes and that the entire *N*-terminus of AS160 is required for efficient interaction with IRAP.

The inhibitory role of AS160-4P depends on its interaction with IRAP

It has previously been shown that an AS160 phosphorylation mutant (AS160 4P) has an inhibitory effect on GLUT4 trafficking (Sano et al., 2003). We next wanted to determine the role of PM versus IRAP binding in this inhibitory role of AS160. Initially we focused on the IRAP binding domain by constructing an AS160 4P mutant disabled for IRAP binding. In contrast to AS160-4P, overexpression of a Pollux-AS160 3P mutant was without effect on insulin-mediated GLUT4 translocation (Fig. 5A). To further confirm these findings we next examined AS160 phosphorylation mutants that displayed a range of IRAP binding efficiencies (Fig. 4B). $AS160_{365\text{-}1299}$-3P, which does not interact with IRAP (Fig. 4B), did not inhibit insulin–mediated GLUT4 translocation (Fig. 5B) while AS160ΔPH 4P, which interacts with IRAP to ~60% the level of wild-type AS160, inhibited insulin-stimulated GLUT4 translocation by 10-20% (Fig. 5C). Conversely, $AS160_{KK215/216AA}$-4P, which interacts with IRAP to ~80-90% of that observed with wild-type AS160, fully retained its inhibitory potential on GLUT4 translocation in the context of a AS160-4P mutant (Fig. 5D). These data indicate that the AS160 interaction with IRAP is necessary for its inhibitory role in retaining GSVs in its intracellular compartment. Conversely, the PM interaction alone does not appear to confer inhibition.

The AS160 PM interaction plays a positive role in GLUT4 translocation

We next wanted to determine the role of the PM interaction of AS160 in GLUT4 trafficking. Because knock down of AS160 has been reported to inhibit insulin-dependent GLUT4 translocation (Brewer et al., 2011; Eguez et al., 2005) we postulated that in addition to its inhibitory role under basal conditions, AS160 may also have a positive regulatory role on GLUT4 trafficking in the presence of insulin. To test this we reasoned that constitutive targeting of AS160 to the PM might replicate its positive role resulting in increased GLUT4 translocation in the absence of insulin. A Flag-AS160 construct containing the myristoylation/palmitoylation PM-targeting signal from Lyn (Lyn-AS160) was expressed in adipocytes. This was highly enriched at the PM as determined by subcellular fractionation and immunofluorescence microscopy (Supp. Figs. 1A &1B). Lyn-AS160 increased PM levels of HA-GLUT4 in non-stimulated cells by ~2 fold and potentiated insulin-dependent GLUT4 translocation at submaximal insulin levels (Fig. 6A). Moreover, the time course of insulin-dependent (1 nM) appearance of GLUT4 at the PM was significantly increased in cells

expressing Lyn-AS160 (Fig. 6B). This increase in HA-GLUT4 translocation in cells expressing Lyn-AS160 was not due to increased GLUT4 expression (Supp. Fig. 3A) and it is not likely due to reduced GLUT4 endocytosis as this would have led to a potentiation of cell surface GLUT4 levels at maximum insulin stimulation (Fig. 6A). One possibility is that because AS160 can form homo-dimers, Lyn-AS160 may have dimerised with endogenous AS160 leading to its accumulation at the PM thus relieving the inhibitory effect of AS160 on intracellular GSVs. However, we did not observe a significant change in the subcellular distribution of endogenous AS160 in cells overexpressing Lyn-AS160 (Supp Fig. 3B). This supports a positive regulatory role for AS160 at the PM in regulating GLUT4 trafficking.

We next determined if increased GLUT4 translocation in Lyn-AS160 expressing cells could be due to altered Akt signaling. Phosphorylation of Akt at Thr308 or Ser473 was comparable in cells expressing Flag-AS160 and Lyn-AS160 in both unstimulated and insulin-stimulated cells (Fig. 6C). Phosphorylation of Akt substrates, Ser21/9 GSK3α/β and pThr1462 TSC2, were also similar in cells expressing Flag-AS160 and Lyn-AS160 (Fig. 6C). Importantly, there was a significant increase in phosphorylation of Lyn-AS160 and also endogenous AS160 at Thr642 under basal conditions compared to cells expressing Flag-AS160 (Fig. 6C & Supp. Fig. 4A). The specific Akt inhibitor MK-2206 (Tan et al., 2011) partially blocked this effect on Lyn-AS160 but totally inhibited phosphorylation of endogenous Thr642 AS160 (Fig. 6C, Supp. Fig. 3C & 3D). A possible explanation for this is that a very small pool of active Akt below the detection limit exists at the PM in unstimulated cells that is unaffected by MK-2206. These data indicate that constitutive targeting of AS160 to the PM is sufficient to facilitate its phosphorylation and enhance GLUT4 translocation in the absence of insulin stimulation and that Lyn-AS160 recruits endogenous AS160 to the PM *via* homo-dimerisation (Dash et al., 2009; Koumanov et al., 2011) facilitating phosphorylation of both proteins. Consistent with this model, endogenous AS160 was co-immunoprecipitated with Lyn-AS160 as well as with wild type Flag-AS160 in 3T3-L1 adipocytes (Supp. Fig. 3E). This likely represents a low proportion of endogenous AS160 that is recruited to the PM because the overall subcellular distribution of endogenous AS160 does not change in cells overexpressing Lyn-AS160 (Supp. Fig. 3B). To test whether targeting AS160 to other membranes could result in its phosphorylation, we expressed a chimera of AS160 fused to GLUT4 (Stockli et al., 2008) in 3T3-L1 adipocytes. Compared to Lyn-AS160, AS160-GLUT4 exhibited low levels of Thr642 phosphorylation in the absence of insulin (Supp. Fig. 3F).

We made use of the knowledge that phosphorylation of endogeneous AS160 can be inhibited by the Akt inhibitor whereas that of the PM-targeted AS160 is less affected under both basal and insulin-stimulated conditions (Fig. 6C), to determine if the potentiating effect of Lyn-AS160 on GLUT4 could be due to increased phosphorylation of endogenous AS160. Cells were

pretreated with MK-2206 followed by insulin. In cells expressing Flag-AS160, both endogenous AS160 and Flag-AS160 were highly phosphorylated upon insulin stimulation and both were robustly inhibited by MK-2206 (Fig. 6D), as was insulin-stimulated GLUT4 translocation (Figs. 6E & 6F). In Lyn-AS160 expressing cells, MK-2206 treatment inhibited phosphorylation of endogenous AS160 in the basal state but it had minimal effect on Lyn-AS160 phosphorylation (Fig. 6D). Inhibition of endogenous AS160 phosphorylation did not affect the potentiating effect of Lyn-AS160 on GLUT4 translocation (Figs. 6E & 6F). Consistent with this, the potentiating effect of Lyn-AS160 on GLUT4 translocation was retained in insulin-stimulated (low dose, 1 nM) cells treated with MK-2206 (Figs. 6E & 6F). A similar trend was observed by measuring glucose uptake in wild type 3T3-L1 adipocytes expressing Lyn-AS160, indicating that this effect is independent of HA-GLUT4 expression (Figs. 6G & 6H). These data indicate that the potentiating effect of Lyn-AS160 on GLUT4 translocation is not due to increased phosphorylation of endogenous AS160 and it is likely associated with phosphorylation of Lyn-AS160 at the PM.

Lyn-AS160 4P mutant inhibits GLUT4 translocation

We next sought to determine if the increase in phosphorylation of AS160 at the PM is required for the potentiating effect on GLUT4 translocation. To test this, the effects of the AS160-4P or Lyn-AS160-4P on GLUT4 trafficking were examined. Lyn-AS160-4P was enriched at the PM as determined by subcellular fractionation and immunofluorescence microscopy (Supp. Fig. 1). Consistent with previous studies (Larance et al., 2005; Ramm et al., 2006; Sano et al., 2003; Zeigerer et al., 2004), AS160-4P inhibited insulin-stimulated HA-GLUT4 translocation to the PM by ~50% compared to cells expressing wild type AS160 (Fig. 7A). We also observed a significant decrease in basal cell surface levels of HA-GLUT4 in cells expressing AS160-4P (Fig. 7A) supporting the hypothesis that non-phosphorylated AS160 retains GLUT4 in its intracellular compartment (Larance et al., 2005; Sano et al., 2003). Whereas Lyn-AS160 increased basal HA-GLUT4 levels (Fig. 7A), this effect was not observed in cells expressing Lyn-AS160-4P. Moreover, Lyn-AS160-4P decreased HA-GLUT4 translocation in insulin-stimulated cells, albeit to a lesser extent to AS160-4P (Fig. 7A).

The myristoylation/palmitoylation domain of Lyn has been described to confer localization to lipid rafts in the PM (Field et al., 1995). To determine if AS160 fulfills its positive regulatory role in lipid rafts we conducted a series of experiments using AS160 fused to the polybasic CAAX domain of Kras (AS160-Kras). This domain has been shown to confer targeting to a non-lipid raft domain in the PM (Roy et al., 1999). Subcellular fractionation and immunofluorescence microscopy verified that AS160-Kras was targeted to the PM (Supp Fig. 1). AS160-Kras and AS160-4P-Kras had similar effects on GLUT4 trafficking to that observed with the cognate Lyn-constructs (Supp.

Figs. 4A & 4B). Hence, these data suggest that AS160 mediates its positive role in GLUT4 trafficking via non-discriminate targeting to the PM.

The positive role of AS160 on GLUT4 translocation does not require a functional GAP.

To determine if the inhibitory effect of PM-targeted AS160-4P is due to its RabGAP function, we mutated the critical arginine residue to alanine in Lyn-AS160 (Lyn-4P-R/A). Lyn-4P-R/A did not inhibit insulin-stimulated HA-GLUT4 translocation indicating the importance of the GAP domain in the inhibitory function (Fig. 7B). Interestingly, cells expressing Lyn-4P-R/A retained the potentiating effect on HA-GLUT4 translocation (Fig. 7B) suggesting that the inactive GAP is required for this function. However, expressing the GAP domain alone at the PM (Lyn-GAP) or the inactive GAP domain (Lyn-GAP R/A) had no effect on GLUT4 translocation (Supp. Fig. 4C), indicating that the potentiating effect is mediated via other domains in AS160, but is inhibited by an active GAP domain.

Finally, we wanted to test the role of 14-3-3 binding in the positive actions of AS160 since this is thought to inhibit AS160 GAP activity (Geraghty et al., 2007; Ramm et al., 2006). An AS160 4P mutant that constitutively binds to 14-3-3 (4PR18) reversed the inhibitory effect of 4P on GLUT4 translocation in adipocytes (Supp Fig. 4D) consistent with previous studies (Ramm et al., 2006). This effect was overcome by mutating two key lysines in the 14-3-3 binding site (Supp. Fig. 4D) that disrupt 14-3-3 binding (4PR18KK) (Ramm et al., 2006). Based on the observation that Lyn-AS160 with an inactive GAP maintains potentiation of GLUT4 translocation (Fig. 7B), we predicted that PM targeting of the constitutive 14-3-3 binding mutant (Lyn-4PR18) would phenocopy the GAP mutant. Consistent with this, overexpression of Lyn-4PR18 in adipocytes potentiates basal GLUT4 levels at the PM, whereas overexpression of a mutant that reverse the constitutive 14-3-3 binding (Lyn-4PR18KK) negate this effect (Fig. 7C). Therefore inactivation of the GAP function of AS160 either by mutating the GAP domain or by 14-3-3 binding positively affects GLUT4 translocation to the plasma membrane.

Discussion

In this study we describe both negative and positive roles for the RabGAP AS160 in GLUT4 trafficking in adipocytes that couple the nutritional state of the cell to GLUT4 translocation via Akt-dependent phosphorylation of this protein. The inhibitory action of AS160, which has been well described (Brewer et al., 2011; Ramm et al., 2006; Sano et al., 2003; Stockli et al., 2008; Zeigerer et al., 2004), involves its interaction with IRAP, and possibly other cargo on GSVs (Jedrychowski et al.) In this case, the AS160 GAP must be active to inhibit a cognate Rab that is required to promote GLUT4 translocation. The positive effect is mediated via an N-terminal domain comprising amino

acids 190-365 in AS160 that confers its localization to the PM. This domain possesses positively charged residues, which are highly conserved in other members of the AS160 subfamily that regulate an interaction between AS160 and cell surface phospholipids. The association of AS160 with the PM plays a positive regulatory role in GLUT4 trafficking and this function relies on AS160 phosphorylation/14-3-3 binding leading to inhibition of AS160 GAP activity.

The mammalian RabGAP family of proteins is comprised of over 50 members (Bernards, 2003). The characteristic feature of all members is a GAP or TBC domain, which co-exists with a range of other domains that presumably encode the unique functions of each family member. AS160 binds to calmodulin via its calmodulin binding domain (Kane and Lienhard, 2005), to 14-3-3 via Akt-dependent phosphorylation (Geraghty et al., 2007; Ramm et al., 2006), to IRAP and other vesicle cargo via an N-terminal domain (Jedrychowski et al.; Peck et al., 2006) and it forms oligomers (Dash et al., 2009; Koumanov et al., 2011). Here we describe another interaction of AS160 involving its N-terminal PH-like domain that binds to phospholipids facilitating association of AS160 with the PM. There are two classes of PH domains: those that bind to specific phospholipids, such as the PH domain of phospholipase C that binds specifically to PI(4,5)P3 (Kutateladze, 2010; Lemmon, 2008); and those that bind more promiscuously to various phosphorylated phospholipids (Kutateladze, 2010; Lemmon, 2008). AS160 would fall into the second class. The PM localization domain in AS160 is highly conserved in different species and it is also present in the AS160 homologue TBC1D1 and the *Drosophila* orthologue Pollux. We show that both TBC1D1 and Pollux associate with the PM to a similar extent as AS160, whereas members of the TBC family lacking this PM association domain have reduced PM association. This indicates that AS160, TBC1D1 and Pollux all share a conserved function to regulate vesicle transport at the PM.

AS160 negatively regulates GLUT4 translocation to the PM by binding to GSVs, inhibiting GTP loading of a Rab on these vesicles and preventing GSV docking to the PM (Larance et al., 2005; Ramm et al., 2006; Sano et al., 2003; Zeigerer et al., 2004). We have previously proposed an additional function for AS160 at the PM, based upon the identification of a high specific activity pool of phosphorylated AS160 at this location in adipocytes (Ng et al., 2010). The identification of an AS160 PM localization motif in the current study provides additional support for this hypothesis. It was difficult to resolve the novel role at the PM from the negative role on GSVs. To circumvent the role of AS160 on GSVs we targeted AS160 to the PM by tagging it with a PM localization motif. Surprisingly, this resulted in increased PM levels of GLUT4 in the absence of insulin (Figs. 6A & 6B). One likely explanation for this positive effect is that PM-targeted AS160 was highly phosphorylated even in the absence of insulin (Fig. 6C & 6D). We propose insulin-independent phosphorylation of PM targeted AS160 is mediated via a small amount of active Akt at this

location. In much the same way that constitutive PM-targeting of Akt leads to its phosphorylation and activation (Kohn et al., 1996a; Kohn et al., 1996b), we propose that recruiting AS160 to the PM is sufficient to increase its phosphorylation by accessing the finite pool of active Akt at the PM.

In view of previous studies suggesting that phosphorylation of AS160 leads to 14-3-3 binding and inhibition of its GAP activity (Ramm et al., 2006), we proposed that the positive effect of AS160 at the PM was linked to abolished GAP activity. Consistent with this, mutations within PM-targeted AS160 that either enhanced 14-3-3 binding or disarmed the GAP activity increased PM GLUT4 levels in insulin's absence (Fig. 7). These data suggest that the basal increase in PM GLUT4 was dependent on inactivation of AS160 GAP activity rather than its phosphorylation. There is clearly an additional role for other domains in the N-terminus of AS160 in this positive effect at the PM because targeting of the inactive GAP domain of AS160 alone to the PM did not increase basal GLUT4 translocation (Supp Fig. 4C). Overexpression of Lyn-AS160 did not change phosphorylation of Akt, GSK3 or TSC2 nor did it change the localization of endogenous AS160 (Fig. 6C). Intriguingly, phosphorylation of endogenous AS160 was also increased following overexpression of Lyn-AS160 (Figs. 6C, Supp Fig. 3D) we suspect due to dimerization of endogenous AS160 with Lyn-AS160 (Supp Fig 3E). This could not, however, explain the positive regulatory role of Lyn-AS160 on GLUT4 trafficking because inhibition of endogenous AS160 phosphorylation did not affect the increase in PM GLUT4 levels (Figs. 6D to 6F). Collectively, this suggests a positive role for AS160 at the PM that requires N-terminal domains in AS160 as well as inactivation of its GAP activity.

The data described above support and extend the well-established negative role of AS160 on GLUT4 trafficking. Notably, loss of function mutations in AS160 that disrupted PM binding, and presumably the positive regulatory role, retained GSV binding and the ability to inhibit GLUT4 trafficking in the context an AS160 phosphorylation mutant (AS160-KK-4P) (Fig 5D).

How can one rationalize both positive and negative regulatory roles for AS160 in GLUT4 trafficking? We propose that AS160 acts as a gatekeeper for GLUT4 translocation to the PM, playing a dual role in this process. In the original model it was proposed that under basal conditions, non-phosphorylated AS160 binds to GSVs via IRAP, preventing docking/fusion with the PM by inactivating a Rab that is required for translocation of GSVs to the PM. Insulin stimulates AS160 phosphorylation and 14-3-3 binding, leading to inactivation of the GAP and GTP-loading of the Rab. Here we extend this model to include an additional positive regulatory role for AS160 at the PM. GSVs, with AS160 bound, move toward the PM and bind to the PM via the PH-like domain at the N-terminus of AS160. If Akt is inactive (without insulin), AS160 will remain non-phosphorylated, the GAP will be active and its cognate Rab inactive thus inhibiting fusion, leading to dissociation of the GSVs from the PM. Consistent with a negative regulatory role of AS160 at

the PM under basal conditions, PM targeted AS160-4P inhibited insulin-stimulated GLUT4 translocation to the PM, suggesting that AS160 can function as an active RabGAP at this location. If on the other hand GSVs, after arrival at the PM, encountered active Akt (plus insulin) this will lead to phosphorylation of AS160, inhibiting of its GAP activity leading to GTP loading of the Rab on GSVs, all while GSVs remain associated with the PM via AS160. We propose that an additive interaction of GSVs with the PM encoded by both AS160 tethering via the PH-like domain and binding of GTP-loaded Rab with cognate PM effectors leads to a high affinity interaction of GSVs with the PM. It is likely that each interaction on its own, as predicted to occur in insulin's absence, will result in a low affinity interaction and rapid dissociation of GSVs from the PM. The dual interaction likely shifts the equilibrium in favour of vesicle fusion as opposed to dissociation. Consistent with this model, knock down of AS160 leads to reduced insulin-stimulated GLUT4 translocation (Brewer et al., 2011; Eguez et al., 2005). Implicit in this model, is that AS160 stays on the vesicle until fusion and its phosphorylation occurs at the PM. It was originally considered that AS160 phosphorylation would occur on GSVs leading to dissociation of AS160 from GSVs in response to insulin (Larance et al., 2005). However, it was subsequently found that dissociation of AS160 from GSVs is not necessary for GLUT4 translocation (Stockli et al., 2008). Furthermore, studies using an *in vitro* reconstitution system showed that AS160 on GSVs isolated from insulin stimulated rat adipocytes does not disassociate while trafficking for fusion with isolated PM (Koumanov et al., 2011). Moreover, the stoichiometry of AS160 phosphorylation when attached to GSVs is much lower than that of PM associated AS160 (Supp. Fig. 3F). Given that Akt is normally activated at the PM (Alessi et al., 1996) and the trafficking of GSVs towards the PM occurs in an Akt-independent manner (van Dam et al., 2005) this might suggest that Akt acts in GLUT4 trafficking at the PM and not at GSVs. The dissociation of AS160 from the GSVs might simply be a consequence of the vesicles fusing with the PM.

In summary, we have mapped out the critical residues for the association of AS160 with phospholipids at the PM and unravel an additional positive role for AS160 in GLUT4 translocation. These data implicate AS160 as a major fork in the pathway that determines the probability that GSVs will either fuse with the PM or recycle back to the cell interior. This is a highly efficient way of coupling the activity of the Rab on the vesicle to the correct location in the cell, to which the vesicle is destined to fuse, and the nutrient status of the cell, which is encoded by the activity state of Akt also found at the same location.

Materials and Method

Cell Culture, retroviral infection and transfection

3T3-L1 fibroblasts (ATCC, Manassas, VA) were cultured and differentiated to adipocytes as described previously (Larance et al., 2005). 3T3-L1 fibroblasts infected with pWZLneo HA-GLUT4 and various pBabepuro-AS160 retroviruses were selected with 2 μg/ml puromycin and 800 μg/ml geneticin in DMEM with 10% fetal calf serum (FCS). Surviving 3T3-L1 fibroblasts were grown to confluence and differentiated into adipocytes. CHO IR/IRS-1 cells (ATCC, Manassas, VA) were cultured in F-12 medium respectively, containing 10% FCS, 800 μg/ml G418, 2 mM L-glutamax, 100 U/L penicillin, and 100 μg/L streptomycin at 37 °C in 10% CO_2. HEK293E cells (ATCC, Manassas, VA) were cultured in DMEM supplemented with 10% FCS, 2 mM L-glutamax, 100 U/L penicillin, and 100 μg/L streptomycin at 37 °C in 10% CO_2. CHO IR/IRS-1 cells, and HEK293E cells were transfected with DNA constructs using Lipofectamine LTX (Invitrogen) or Lipofectamine 2000 (Invitrogen) respectively according to the manufacturer's instructions.

Western Blotting and Immunoprecipitation

Following treatments, cells were washed twice with ice-cold PBS and solubilized in 2% SDS in PBS containing phosphatase and protease inhibitor. Insoluble material was removed by centrifugation at 18,000 × g for 10 min. Proteins were separated by SDS-PAGE and proteins transferred to polyvinylidene difluoride membranes. Membranes were blocked using 5% skim milk in Tris-buffered saline (TBS) and immunoblotted with the relevant antibodies overnight at 4 °C in blocking buffer (5% BSA, 0.1% Tween in TBS). Membranes were washed and incubated with horseradish peroxidase-labeled secondary antibodies and detected by SuperSignal West Pico chemiluminescent substrate. In some cases, IR dye 700 or 800 conjugated secondary antibodies were used and scanned at the 700 nm and 800 nm channel using the Odyssey IR imager. Quantification of protein levels was performed using Odyssey IR imaging software or ImageJ software.

Following the indicated treatment, cells were washed with ice-cold PBS and solubilized in NP-40 buffer (50 mm Tris-HCl, pH 7.5, 150 mm NaCl, 1% NP-40, 1 mm EDTA, and 10% glycerol) containing protease and phosphatase inhibitors. Cell lysates were homogenized and centrifuged at 18,000 × g for 20 min at 4 °C. One mg of cell lysates were incubated overnight at 4 °C with 2 μg of FLAG antibody with protein G-Sepharose beads. Immunoprecipitates were washed with ice-cold NP-40 buffer prior to western blotting.

GST-IRAP Pull Down

Cell lysates isolated from HEK293E cells transfected with various constructs of AS160 were incubated for 2 h at 4°C with glutathione Sepharose beads bound with various GST-IRAP proteins purified from *E. Coli*. Beads were washed extensively prior to processing for western blotting.

Lipid Blot

PIP microstrips (Echelon) were processed according to the manufacturer's instructions with some modification. Briefly, strips were blocked with 5% non-fat milk in TBS-0.1% Tween buffer for 1 h prior to overnight incubation with 1 mg/ml of purified GST-protein from *E.Coli* in TBS-0.1% Tween containing 2% BSA. After extensive washing, strips were incubated with anti-mouse GST antibody, washed and probed with anti-mouse HRP. Secondary antibody was detected using ECL as described in western blotting analysis.

Cationic Silica Isolation of Plasma Membrane and Subcellular Fractionation

Cationic Silica Isolation of Plasma Membrane and Subcellular Fractionation were performed as previously described (Larance et al., 2005).

Live cell TIRF Microscopy

3T3-L1 adipocytes were electroporated as described previously (Stockli et al., 2008). Live cell TIRF microscopy was performed using a Zeiss Axiocam MRm equipped with a heated stage set at 37°C. Cells were randomly selected by bright field illumination prior to TIRF imaging, and images were analyzed with ImageJ software.

Immunofluorescence Microscopy

3T3-L1 adipocytes were cultured and differentiated as described above on glass coverslips. Cells were fixed with 3% paraformaldehyde in PBS and free aldehyde groups were quenched with 50 mM glycine in PBS. The cells were processed for immunolabeling by permeabilization and labeling in PBS containing 0.1% saponin and 2% BSA using standard procedures. Primary antibodies were detected with CY2-conjugated secondary antibodies. Optical sections were analyzed by epifluorescence microscopy on a Leica inverted microscope. The contrast was adjusted for all images with the same settings.

Quantitative GLUT4 Translocation Assay

HA-GLUT4 translocation to the plasma membrane was measured as described previously (Govers et al., 2004).

2-Deoxyglucose Uptake Assay

2-deoxyglucose uptake into 3T3-L1 adipocytes was performed as described previously (van Dam et al., 2005).

Statistical Analysis

Data are expressed as means ± standard deviation (SD) or ± standard error (SE). *p* values were calculated by two tailed Student's t test using Microsoft Excel.

Acknowledgements

We thank Dr. Morris Birnbaum (University of Pennsylvania, USA) for providing the Pollux cDNA. The Akt inhibitor, MK-2206, was generously provided by Dr. Dario Alessi (University of Dundee, UK). This work was supported by grants from the National Health and Medical Research Council (NHMRC) of Australia. D.E.J. is an NHMRC Senior Principal Research Fellow.

Figure Legends

Figure 1: The N-terminus of AS160 is important for PM localization and IRAP binding.

(A) Schematic diagrams of full-length (FL) and different fragments of human AS160 proteins used in this study. Numbers indicate amino acid boundaries. Domain nomenclature: Phosphotyrosine binding domain (PTB); Calmodulin-binding domain (CaM BD); Rab GTPase activating protein domain (Rab GAP).

(B) HEK293E cells were transfected with Flag-tagged $AS160_{1-924}$, $AS160_{719-1299}$, and FL AS160. Plasma membrane (PM) fractions were isolated using the cationic silica isolation method. The total cell lystates (TCL) and the PM fractions were blotted with Flag, GAPDH or Syntaxin 4 antibodies.

(C-D) Quantification of PM localization of Flag-tagged AS160 proteins. Flag-tagged AS160 at the TCL and PM were normalized to GAPDH and Syntaxin 4 levels respectively. The amount of Flag-tagged AS160 at the PM was expressed as a ratio of PM/TCL relative to FL AS160. (C) Results are displayed as means ±S.D. ($n = 2$). (D) Results are displayed as means ±S.E. *$p<0.05$, **$p<0.01$, FL AS160 versus different AS160 fragments, Student's t-test. ($n = 3$).

(E) Schematic diagrams of different cytosolic mutants of IRAP. GST-IRAP pull down of Flag-tagged AS160. HEK293E cells were transfected with Flag-tagged AS160, and the lysates (SM) was passed through sepharose beads containing different GST-tagged IRAP truncation mutants. The pull downs were washed extensively and immunoblotted with Flag antibody.

(F) GST-$IRAP_{1-58}$ pull down (PD) of HEK293E cells transfected with different Flag-tagged AS160. The binding of Flag-tagged AS160 onto GST-$IRAP_{1-58}$ and $IRAP_{1-58AA}$ was quantified. Interaction of AS160 fragments were quantified by subtracting the binding of Flag-tagged AS160 on GST-IRAP from that of GST-$IRAP_{1-58AA}$. The amount of Flag-tagged AS160 bound to GST-$IRAP_{1-58}$ was expressed as a ratio of PD/TCL relative to FL AS160. Results are displayed as means ±S.D *$p<0.05$, **$p<0.01$, FL AS160 versus different AS160 fragments, Student's t-test. ($n = 3$).

Figure 2: Amino acid residues 190-365 of AS160 is important for PM targeting.

(A-C) HEK293E cells were transfected with different Flag-tagged AS160 constructs. (A) The amount of Flag-tagged AS160 at the PM was expressed as a ratio of PM/TCL relative to $AS160_{190-365}$. Results are displayed as means ±S.E. *$p<0.05$, **$p<0.01$, $AS160_{190-365}$ versus different AS160 fragments, Student's t-test. ($n = 3$-6). (B) Results are displayed as means ±S.E. *$p<0.05$, **$p<0.01$, FL AS160 versus different AS160 fragments, Student's t-test. ($n = 3$) (C) Quantification of PM localization of Flag-tagged AS160 proteins and other TBC

members in HEK293E cells. The amount of Flag-tagged TBC proteins at the PM was expressed as a ratio of PM/TCL relative to FL AS160. Results are displayed as means ±S.E. *p<0.05, FL AS160 versus different TBC1D members Student's t-test. (n = 3).

(D) 3T3-L1 adipocytes were electroporated with different EGFP-tagged AS160 truncation mutants and imaged using live-cell TIRFM and epifluorescence. Scale bar = 10 μm.

(E) Fluorescence intensity in the TIRF zone was normalized to total cellular fluorescence, measured *via* epifluorescence. Results are displayed as means ±S.D *p<0.05, **p<0.01. 40 cells were analyzed in each condition.

(F) CHO IR/IRS-1 cells were transfected with various chimeras of ΔPH Akt1 fusion proteins. Cells were serum-starved for 2 h before harvesting. Total cell lysates were subjected to western blot analysis with pThr308 Akt, pSer473 Akt, and total Akt antibodies.

(G) Quantification of relative Akt phosphorylation normalized to total Akt from panel (F). $AS160_{190\text{-}365}$ΔPHAkt1 versus different AS160ΔPHAkt1 chimeras. (n = 4). Results are displayed as means ±S.D *p<0.05, **p<0.01.

Figure 3: $AS160_{190\text{-}365}$ binds acidic phospholipids through two consecutive lysine residues.

(A) HEK293E cells were transfected with Flag-tagged $AS160_{1\text{-}190}$, $AS160_{190\text{-}365}$ and $AS160_{190\text{-}365}$ carrying different point mutations ($AS160_{190\text{-}365\ K209A}$, $AS160_{190\text{-}365\ KK215/216AA}$, $AS160_{190\text{-}365\ K228A}$, and $AS160_{190\text{-}365\ R236A}$). The amount of Flag-tagged AS160 at the PM was expressed as a ratio of PM/TCL relative to $AS160_{190\text{-}365}$. Results are displayed as means ±S.E. **p<0.01, $AS160_{190\text{-}365}$ versus different AS160 constructs, Student's t-test. (n = 3).

(B) 3T3-L1 adipocytes were electroporated with different EGFP-tagged AS160 mutants and imaged using live-cell TIRFM and epifluorescence. Fluorescence intensity in the TIRF zone was normalized to total cellular fluorescence, measured *via* epifluorescence. Results are displayed as means ±S.D **p<0.01. 60 cells were analyzed in each condition.

(C) Lipid binding of GST-AS160 fusion proteins analyzed with protein-lipid overlay assays. Purified GST-AS160 fusion proteins shown by Coomassie staining of SDS-PAGE gel and western blotting with GST antibodies. The GST-AS160 fusion proteins were incubated with Echelon lipid strips and the interactions were revealed with anti-GST antibodies and chemiluminescence. Abbreviations: LPA, Lysophosphatidic Acid; SIP, Sphingosine-1-phosphate; LPC, Lysophosphocholine; PI, Phosphatidylinositol; PI3P, Phosphatidylinositol 3-phosphate; PI4P, Phosphatidylinositol 4-phosphate; PI5P, Phosphatidylinositol 5-phosphate; $PI(3,4)P_2$, Phosphatidylinositol (3,4)-bisphosphate; $PI(3,5)P_2$, Phosphatidylinositol (3,5)-bisphosphate; $PI(4,5)P_2$, Phosphatidylinositol (4,5)-bisphosphate; $PI(3,4,5P_3$, Phosphatidylinositol (3,4,5)-trisphosphate; PE, Phosphatidylethanolamine; PA, Phosphatidic Acid; PS, Phosphatidylserine; PC, Phosphatidylcholine.

(D) Quantification of PM localization of Flag-tagged AS160 proteins in HEK293E cells. The amount of Flag-tagged AS160 at the PM was expressed as a ratio of PM/TCL relative to FL AS160. Results are displayed as means ±S.E. *p<0.05, FL AS160 versus different AS160 fragments, Student's t-test. (n = 3).

Figure 4: AS160 interacts with PM and IRAP via a distinct mechanism.

(A-C) $GST\text{-}IRAP_{1\text{-}58}$ pull down (PD) of HEK293E cells transfected with different Flag-tagged AS160. (A) Total cell lysates (TCL) and pull down (PD) were blotted with Flag antibody. (B) The binding of Flag-tagged AS160 onto $GST\text{-}IRAP_{1\text{-}58}$ and $GST\text{-}IRAP_{1\text{-}58AA}$ was quantified. Interaction of AS160 fragments were quantified by subtracting the binding of Flag-tagged AS160 on GST-IRAP from that of $GST\text{-}IRAP_{1\text{-}58AA.}$ Binding of Flag-tagged AS160 . The amount of Flag-tagged AS160 bound to $GST\text{-}IRAP_{1\text{-}58}$ was expressed as a ratio of PD/TCL relative to FL AS160. Results are displayed as means ±S.D *p<0.05, **p<0.01, FL AS160 versus different AS160 fragments, Student's t-test. (n = 3). (C) Quantification of

GST-IRAP$_{1-58}$ pull down of Flag-tagged AS160 proteins and other TBC members in HEK293E cells. The amount of Flag-tagged TBC members bound to GST-IRAP$_{1-58}$ was expressed as a ratio of PD/TCL relative to FL AS160.Results are displayed as means ±S.D. *p<0.05, **p<0.01, FL AS160 versus different TBC1D members Student's t-test. (n = 3).

(D) HEK293E cells were transfected with Flag-tagged AS160, Flag-tagged Pollux and Flag-tagged Pollux-AS160 chimera. The amount of Flag-tagged AS160/Pollux at the PM was expressed as a ratio of PM/TCL relative to FL AS160. Results are displayed as means ±S.D. **p<0.01, FL AS160 versus different AS160/Pollux constructs, Student's t-test. (n = 3).

(E) GST-IRAP$_{1-58}$ pull down (PD) of HEK293E cells transfected with different Flag-tagged AS160/Pollux constructs. The amount of Flag-tagged AS160/Pollux bound to GST-IRAP$_{1-58}$ was expressed as a ratio of PD/TCL relative to FL AS160.Results are displayed as means ±S.D. **p<0.01, FL AS160 versus different AS160/Pollux constructs Student's t-test. (n = 3).

Figure 5: The inhibitory effect of AS160-4P on GLUT4 trafficking correlates with the degree of IRAP interaction.

(A-D) 3T3-L1 adipocytes expressing Flag-tagged AS160 (AS160WT) or various Flag-tagged AS160 mutants were serum-starved for 2 h and stimulated with or without 100 nM insulin for 20 min. The amount of HA-GLUT4 at the PM was determined by anti HA fluorescence immunolabeling of non-permeabilised cells, and expressed as percentage of total cellular HA-GLUT4, determined by labeling of permeabilised cells. Results are displayed as means ±S.D. *p<0.05, **p<0.01, Student's t-test. (n = 3).

Figure 6: AS160 targeted to the PM increases basal Thr642 phosphorylation, GLUT4 translocation and glucose uptake.

(A) Dose response of HA-GLUT4 translocation in 3T3-L1 adipocytes expressing Flag-tagged AS160 and Flag-tagged Lyn-AS160. HA-GLUT4 and Flag-tagged AS160 expressing 3T3-L1 adipocytes were serum-starved for 2 h and stimulated with indicated dose of insulin for 10 min. The amount of HA-GLUT4 at the PM was determined by anti HA fluorescence immunolabeling of non-permeabilised cells, and expressed as percentage of total cellular HA-GLUT4, determined by labeling of permeabilised cells. Results are displayed as means ±S.E. *p<0.05, **p<0.01, Student's t-test. (n = 4).

(B) Time course of HA-GLUT4 translocation in 3T3-L1 adipocytes expressing Flag-tagged AS160 and Flag-tagged Lyn-AS160. HA-GLUT4 and Flag-tagged AS160 expressing 3T3-L1 adipocytes were serum-starved for 2 h and stimulated with 1 nM for the indicated time points. Results are displayed as means ±S.E. *p<0.05, **p<0.01, Student's t-test. (n = 3).

(C) Flag-tagged AS160 expressing 3T3-L1 adipocytes were serum-starved for 2 h. Cells were treated with either 0.1% DMSO (D) or 10 μM MK-2206 (M) for 30 min before 100 nM insulin stimulation. Total cell lysates were subjected to western blot analysis with pThr642 AS160, total AS160, pThr308 Akt, pSer473 Akt, total Akt, pSer21/9 GSK3α/β, pThr1462 TSC2 or 14-3-3β antibodies.

(D) Flag-tagged AS160 expressing 3T3-L1 adipocytes were serum-starved for 2 h. Cells were treated with either 0.1% DMSO (D), 1 μM MK-2206 (MK) or 10 μM MK-2206 for 30 min before 1 nM or 100 nM insulin stimulation. Total cell lysates were subjected to western blot analysis with pThr642 AS160, total AS160, pThr308 Akt, pSer473 Akt or total Akt antibodies.

(E-F) HA-GLUT4 translocation in 3T3-L1 adipocytes expressing Flag-tagged AS160 or Flag-tagged Lyn-AS160. Cells were serum-starved for 2 h and were treated with either 0.1% DMSO (D), 1 μM MK-2206 (MK) or 10 μM MK-2206 for 30 min before 1 nM (E) or 100

nM (F) insulin stimulation. Results are displayed as means ±S.D. *p<0.05, **p<0.01, Student's t-test. (n = 3).

(G-H) Glucose uptake in 3T3-L1 adipocytes expressing Flag-tagged AS160 or Flag-tagged Lyn AS160. Cells were serum-starved for 2 h and treated with either 0.1% DMSO, 1 μM MK-2206 or 10 μM MK-2206 for 30 min before (H) with or (G) without 1 nM insulin stimulation. Results are displayed as means ±S.E. *p<0.05, Student's t-test. (n = 3).

Figure 7: The potentiating effect of Lyn-AS160 on GLUT4 translocation does not require active GAP.

(A-C) 3T3-L1 adipocytes expressing HA-GLUT4 and various Flag-tagged AS160 mutants were serum-starved for 2 h and stimulated with 100 nM insulin for 20 min. (A-B) Results are displayed as means ±S.E. *p<0.05, **p<0.01, Student's t-test. (n = 4). (C) Results are displayed as means ±S.D. *p<0.05, Student's t-test. (n = 6).

Supplementary Figure 1. Subcellular localization of AS160 constructs.

(A) 3T3-L1 adipocytes expressing different AS160 constructs were fractionated to obtain different subcellular fractions, TCL, cytosol (cyt), high density microsomes (HDM), low density microsomes (LDM), plasma membranes (PM), and mitochondria/nuclei (M/N). Fractions were blotted with Flag antibody.

(B) 3T3-L1 adipocytes retrovirally expressing Flag-tagged Lyn-AS160 or Flag-tagged AS160-Kras constructs were fixed and immunolabelled with Flag antibody followed by Cy2-conjugated secondary antibody.

Supplementary Figure 2: Multiple alignments of amino acid residues 190-239 of human AS160 with TBC1D1 and Pollux.

Multiple-sequence alignments of residues 190-239 of human AS160 with its different species and close homologues, TBC1D1, and Pollux using Clustal W version 2.012. Numbers indicate amino acid. "*" indicates fully conserved residues; ":" indicates highly conserved residues; "." indicates weakly conserved residues. Residues that are boxed are conserved lysine or arginine residues that are mutated to alanines and analyzed.

Supplementary Figure 3:

(A) 3T3-L1 adipocytes retrovirally expressing Flag-tagged Lyn-AS160 or AS160 were harvested and cell lysates were blotted for GLUT4 or tubulin antibodies.

(B) Subcellular fractionation of untransfected 3T3-L1 adipocytes or 3T3-L1 adipocytes expressing Lyn-AS160. Total cell lysates (TCL), cytosol (cyt), high density microsomes (HDM), low density microsomes (LDM), plasma membranes (PM), and mitochondria/nuclei (M/N). Fractions were immunoblotted for total AS160.

(C) Quantification of pThr642 AS160 as shown in Fig. 6C for basal Flag-tagged AS160. Results are displayed as means ±S.E. *p<0.05, DMSO versus MK-2206 treated cells, Student's t-test. (n = 3).

(D) Quantification of pThr642 AS160 as shown in Fig. 6C for endogenous AS160. Results are displayed as means ±S.E. *p<0.05, DMSO versus MK-2206 treated cells, Student's t-test. (n = 3).

(E) Untransfected 3T3-L1 adipocytes or 3T3-L1 adipocytes expressing Flag-tagged AS160 were serum-starved for 2 h (B) and treated with 100 nM insulin for 20 min (I). Total cell lysates

(TCL) were harvested and immunoprecipitated using Flag antibodies. The TCL and Flag immunoprecipitates (IP) were subjected to western blot analysis using total AS160 antibody.

(F) 3T3-L1 adipocytes were electroporated with various AS160 chimeras. Total cell lysates were isolated and immunoblotted for pThr642 AS160 and total AS160 antibodies.

Supplementary Figure 4: HA-Glut4 translocation assays in 3T3-L1 adipocytes retrovirally infected with different AS160 mutants.

(A) Time course of HA-GLUT4 translocation in 3T3-L1 adipocytes expressing Flag-tagged AS160 and Flag-tagged AS160-Kras. Cells were serum-starved for 2 h and stimulated with 1 nM for the indicated times. Results are displayed as means ±S.D. (n = 2).

(B-D) 3T3-L1 adipocytes expressing HA-GLUT4 and various Flag-tagged AS160 mutants were serum-starved for 2 h and stimulated with 100 nM insulin for 20 min. (B) Results are displayed as means ±S.E. *p<0.05, **p<0.01, Student's t-test. (n = 4). (C) Results are displayed as means ±S.D. *p<0.05, Student's t-test. (n = 3). (D) Results are displayed as means ±S.D. *p<0.05, **p<0.01, Student's t-test. (n = 5).

References

Alessi, D.R., Andjelkovic, M., Caudwell, B., Cron, P., Morrice, N., Cohen, P., and Hemmings, B.A. (1996). Mechanism of activation of protein kinase B by insulin and IGF-1. EMBO J *15*, 6541-6551.

Bernards, A. (2003). GAPs galore! A survey of putative Ras superfamily GTPase activating proteins in man and Drosophila. Biochim Biophys Acta *1603*, 47-82.

Brewer, P.D., Romenskaia, I., Kanow, M.A., and Mastick, C.C. (2011). Loss of AS160 Akt substrate causes Glut4 protein to accumulate in compartments that are primed for fusion in basal adipocytes. J Biol Chem *286*, 26287-26297.

Chen, S., Murphy, J., Toth, R., Campbell, D.G., Morrice, N.A., and Mackintosh, C. (2008). Complementary regulation of TBC1D1 and AS160 by growth factors, insulin and AMPK activators. Biochem J *409*, 449-459.

Dash, S., Sano, H., Rochford, J.J., Semple, R.K., Yeo, G., Hyden, C.S., Soos, M.A., Clark, J., Rodin, A., Langenberg, C., *et al.* (2009). A truncation mutation in TBC1D4 in a family with acanthosis nigricans and postprandial hyperinsulinemia. Proc Natl Acad Sci U S A *106*, 9350-9355.

Eguez, L., Lee, A., Chavez, J.A., Miinea, C.P., Kane, S., Lienhard, G.E., and McGraw, T.E. (2005). Full intracellular retention of GLUT4 requires AS160 Rab GTPase activating protein. Cell Metab *2*, 263-272.

Field, K.A., Holowka, D., and Baird, B. (1995). Fc epsilon RI-mediated recruitment of p53/56lyn to detergent-resistant membrane domains accompanies cellular signaling. Proc Natl Acad Sci U S A *92*, 9201-9205.

Geraghty, K.M., Chen, S., Harthill, J.E., Ibrahim, A.F., Toth, R., Morrice, N.A., Vandermoere, F., Moorhead, G.B., Hardie, D.G., and MacKintosh, C. (2007). Regulation of multisite phosphorylation and 14-3-3 binding of AS160 in response to IGF-1, EGF, PMA and AICAR. Biochem J *407*, 231-241.

Govers, R., Coster, A.C., and James, D.E. (2004). Insulin increases cell surface GLUT4 levels by dose dependently discharging GLUT4 into a cell surface recycling pathway. Mol Cell Biol *24*, 6456-6466.

Hausdorff, S.F., Fingar, D.C., Morioka, K., Garza, L.A., Whiteman, E.L., Summers, S.A., and Birnbaum, M.J. (1999). Identification of wortmannin-sensitive targets in 3T3-L1 adipocytes. DissociationoOf insulin-stimulated glucose uptake and glut4 translocation. J Biol Chem *274*, 24677-24684.

Jedrychowski, M.P., Gartner, C.A., Gygi, S.P., Zhou, L., Herz, J., Kandror, K.V., and Pilch, P.F. Proteomic analysis of GLUT4 storage vesicles reveals LRP1 to be an important vesicle component and target of insulin signaling. J Biol Chem *285*, 104-114.

Kane, S., and Lienhard, G.E. (2005). Calmodulin binds to the Rab GTPase activating protein required for insulin-stimulated GLUT4 translocation. Biochem Biophys Res Commun *335*, 175-180.

Kane, S., Sano, H., Liu, S.C., Asara, J.M., Lane, W.S., Garner, C.C., and Lienhard, G.E. (2002). A method to identify serine kinase substrates. Akt phosphorylates a novel adipocyte protein with a Rab GTPase-activating protein (GAP) domain. J Biol Chem *277*, 22115-22118.

Kohn, A.D., Summers, S.A., Birnbaum, M.J., and Roth, R.A. (1996a). Expression of a constitutively active Akt Ser/Thr kinase in 3T3-L1 adipocytes stimulates glucose uptake and glucose transporter 4 translocation. J Biol Chem *271*, 31372-31378.

Kohn, A.D., Takeuchi, F., and Roth, R.A. (1996b). Akt, a pleckstrin homology domain containing kinase, is activated primarily by phosphorylation. J Biol Chem *271*, 21920-21926.

Koumanov, F., Richardson, J.D., Murrow, B.A., and Holman, G.D. (2011). AS160 phosphotyrosine-binding domain constructs inhibit insulin-stimulated GLUT4 vesicle fusion with the plasma membrane. J Biol Chem *286*, 16574-16582.

Kutateladze, T.G. (2010). Translation of the phosphoinositide code by PI effectors. Nat Chem Biol *6*, 507-513.

Larance, M., Ramm, G., Stockli, J., van Dam, E.M., Winata, S., Wasinger, V., Simpson, F., Graham, M., Junutula, J.R., Guilhaus, M., and James, D.E. (2005). Characterization of the role of the Rab GTPase-activating protein AS160 in insulin-regulated GLUT4 trafficking. J Biol Chem *280*, 37803-37813.

Lemmon, M.A. (2008). Membrane recognition by phospholipid-binding domains. Nat Rev Mol Cell Biol *9*, 99-111.

Marchler-Bauer, A., Anderson, J.B., Chitsaz, F., Derbyshire, M.K., DeWeese-Scott, C., Fong, J.H., Geer, L.Y., Geer, R.C., Gonzales, N.R., Gwadz, M.*, et al.* (2009). CDD: specific functional annotation with the Conserved Domain Database. Nucleic Acids Res *37*, D205-210.

Miinea, C.P., Sano, H., Kane, S., Sano, E., Fukuda, M., Peranen, J., Lane, W.S., and Lienhard, G.E. (2005). AS160, the Akt substrate regulating GLUT4 translocation, has a functional Rab GTPase-activating protein domain. Biochem J *391*, 87-93.

Ng, Y., Ramm, G., Burchfield, J.G., Coster, A.C., Stockli, J., and James, D.E. (2010). Cluster analysis of insulin action in adipocytes reveals a key role for Akt at the plasma membrane. J Biol Chem *285*, 2245-2257.

Peck, G.R., Chavez, J.A., Roach, W.G., Budnik, B.A., Lane, W.S., Karlsson, H.K., Zierath, J.R., and Lienhard, G.E. (2009). Insulin-stimulated phosphorylation of the Rab GTPase-activating protein TBC1D1 regulates GLUT4 translocation. J Biol Chem *284*, 30016-30023.

Peck, G.R., Ye, S., Pham, V., Fernando, R.N., Macaulay, S.L., Chai, S.Y., and Albiston, A.L. (2006). Interaction of the Akt substrate, AS160, with the glucose transporter 4 vesicle marker protein, insulin-regulated aminopeptidase. Mol Endocrinol *20*, 2576-2583.

Ramm, G., Larance, M., Guilhaus, M., and James, D.E. (2006). A role for 14-3-3 in insulin-stimulated GLUT4 translocation through its interaction with the RabGAP AS160. J Biol Chem *281*, 29174-29180.

Roach, W.G., Chavez, J.A., Miinea, C.P., and Lienhard, G.E. (2007). Substrate specificity and effect on GLUT4 translocation of the Rab GTPase-activating protein Tbc1d1. Biochem J *403*, 353-358.

Roy, S., Luetterforst, R., Harding, A., Apolloni, A., Etheridge, M., Stang, E., Rolls, B., Hancock, J.F., and Parton, R.G. (1999). Dominant-negative caveolin inhibits H-Ras function by disrupting cholesterol-rich plasma membrane domains. Nat Cell Biol *1*, 98-105.

Sano, H., Kane, S., Sano, E., Miinea, C.P., Asara, J.M., Lane, W.S., Garner, C.W., and Lienhard, G.E. (2003). Insulin-stimulated phosphorylation of a Rab GTPase-activating protein regulates GLUT4 translocation. J Biol Chem *278*, 14599-14602.

Sarbassov, D.D., Guertin, D.A., Ali, S.M., and Sabatini, D.M. (2005). Phosphorylation and regulation of Akt/PKB by the rictor-mTOR complex. Science *307*, 1098-1101.

Stockli, J., Davey, J.R., Hohnen-Behrens, C., Xu, A., James, D.E., and Ramm, G. (2008). Regulation of glucose transporter 4 translocation by the Rab guanosine triphosphatase-activating protein AS160/TBC1D4: role of phosphorylation and membrane association. Mol Endocrinol *22*, 2703-2715.

Tan, S.X., Ng, Y., and James, D.E. (2011). Next generation Akt inhibitors provide greater specificity-effects on glucose metabolism in adipocytes. Biochem J.

van Dam, E.M., Govers, R., and James, D.E. (2005). Akt activation is required at a late stage of insulin-induced GLUT4 translocation to the plasma membrane. Mol Endocrinol *19*, 1067-1077.

van der Geer, P., and Pawson, T. (1995). The PTB domain: a new protein module implicated in signal transduction. Trends Biochem Sci *20*, 277-280.

Whiteman, E.L., Cho, H., and Birnbaum, M.J. (2002). Role of Akt/protein kinase B in metabolism. Trends Endocrinol Metab *13*, 444-451.

Yan, K.S., Kuti, M., and Zhou, M.M. (2002). PTB or not PTB -- that is the question. FEBS Lett *513*, 67-70.

Zeigerer, A., McBrayer, M.K., and McGraw, T.E. (2004). Insulin stimulation of GLUT4 exocytosis, but not its inhibition of endocytosis, is dependent on RabGAP AS160. Mol Biol Cell *15*, 4406-4415.

Figure 1:

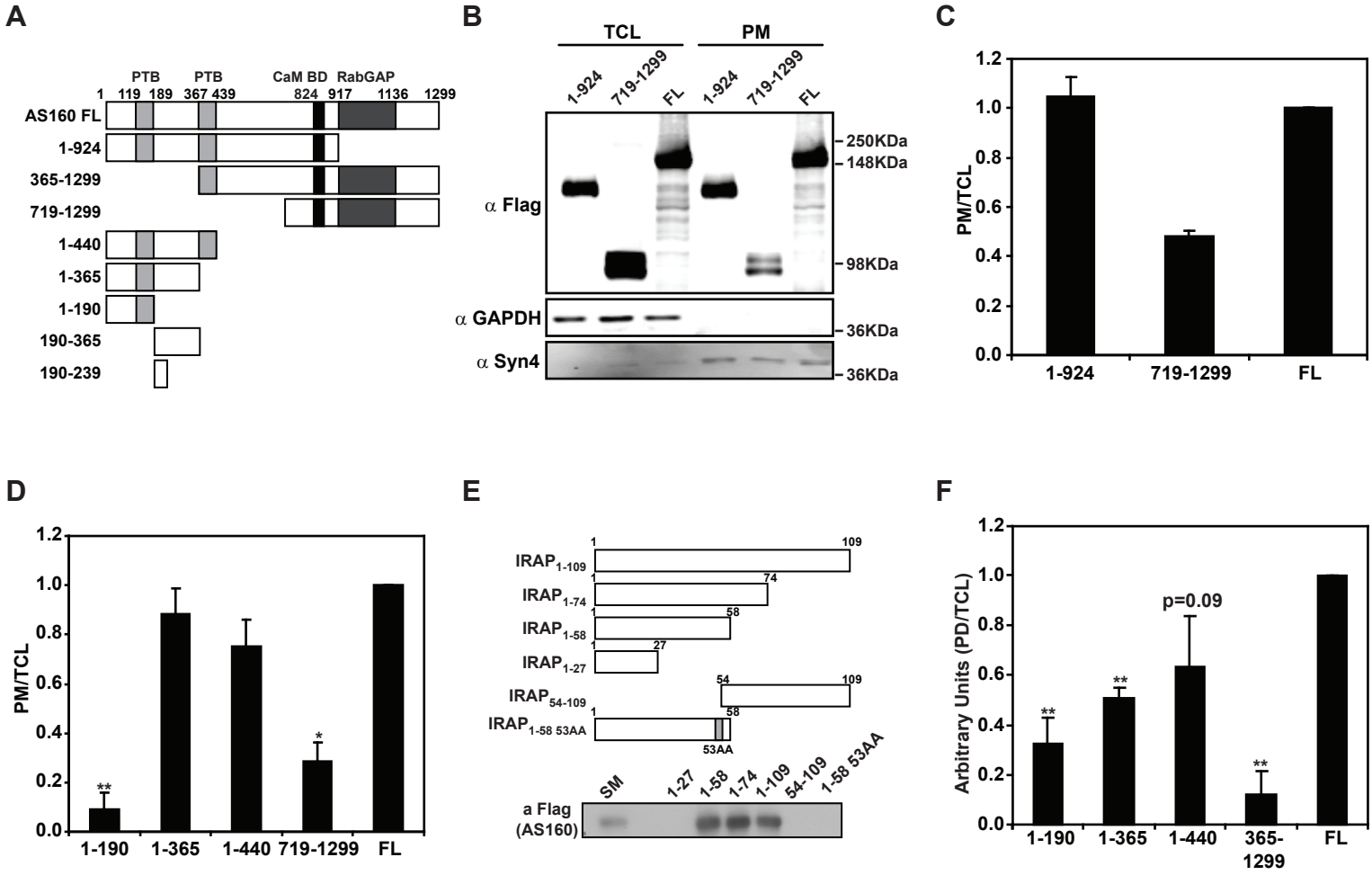
A
PTB
PTB
CaM BD
RabGAP
1
119
189
367
439
824
917
1136
1299
AS160 FL
1-924
365-1299
719-1299
1-440
1-365
1-190
190-365
190-239
B
TCL
PM
1-924
719-1299
FL
1-924
719-1299
FL
250KDa
148KDa
98KDa
36KDa
36KDa
α Flag
α GAPDH
α Syn4
C
PM/TCL
1.2
1.0
0.8
0.6
0.4
0.2
0.0
1-924
719-1299
FL
D
PM/TCL
1.2
1.0
0.8
0.6
0.4
0.2
0.0
**
*
1-190
1-365
1-440
719-1299
FL
E
IRAP1-109
IRAP1-74
IRAP1-58
IRAP1-27
IRAP54-109
IRAP1-58 53AA
1
109
74
58
27
54
53AA
SM
1-27
1-58
1-74
1-109
54-109
1-58 53AA
a Flag
(AS160)
F
Arbitrary Units (PD/TCL)
1.2
1.0
0.8
0.6
0.4
0.2
0.0
**
**
p=0.09
**
1-190
1-365
1-440
365-
1299
FL

Figure 2:

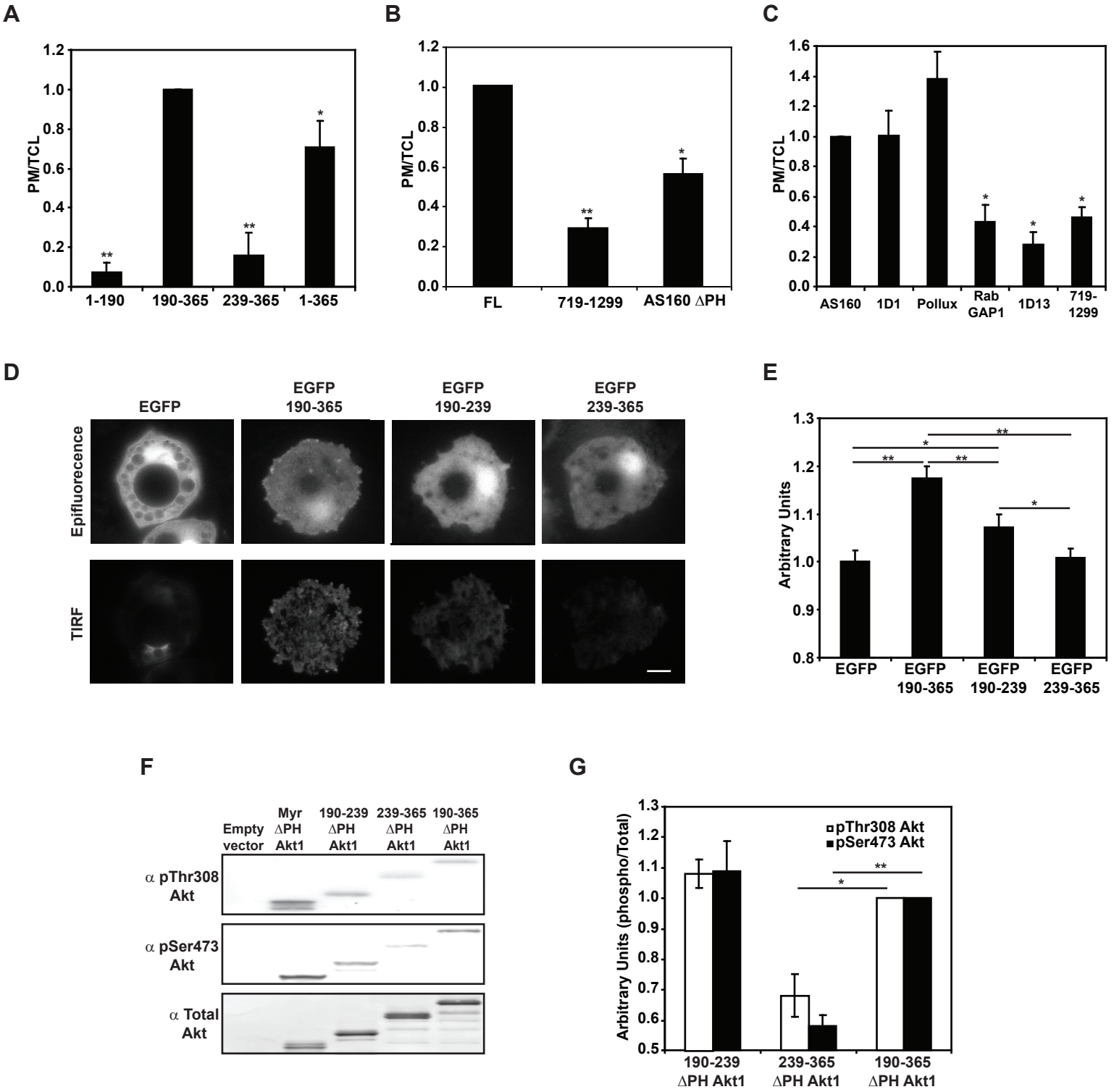
A
PM/TCL
1.2
1.0
0.8
0.6
0.4
0.2
0.0
**
**
*
1-190
190-365
239-365
1-365
B
PM/TCL
1.2
1.0
0.8
0.6
0.4
0.2
0.0
**
*
FL
719-1299
AS160 ΔPH
C
PM/TCL
1.6
1.4
1.2
1.0
0.8
0.6
0.4
0.2
0.0
*
*
*
AS160
1D1
Pollux
Rab GAP1
1D13
719-1299
D
EGFP
EGFP 190-365
EGFP 190-239
EGFP 239-365
Epifluorecence
TIRF
E
Arbitrary Units
1.3
1.2
1.1
1.0
0.9
0.8
**
*
**
**
*
EGFP
EGFP 190-365
EGFP 190-239
EGFP 239-365
F
Empty vector
Myr ΔPH Akt1
190-239 ΔPH Akt1
239-365 ΔPH Akt1
190-365 ΔPH Akt1
α pThr308 Akt
α pSer473 Akt
α Total Akt
G
Arbitrary Units (phospho/Total)
1.3
1.2
1.1
1.0
0.9
0.8
0.7
0.6
0.5
pThr308 Akt
pSer473 Akt
**
*
190-239 ΔPH Akt1
239-365 ΔPH Akt1
190-365 ΔPH Akt1

Figure 3:

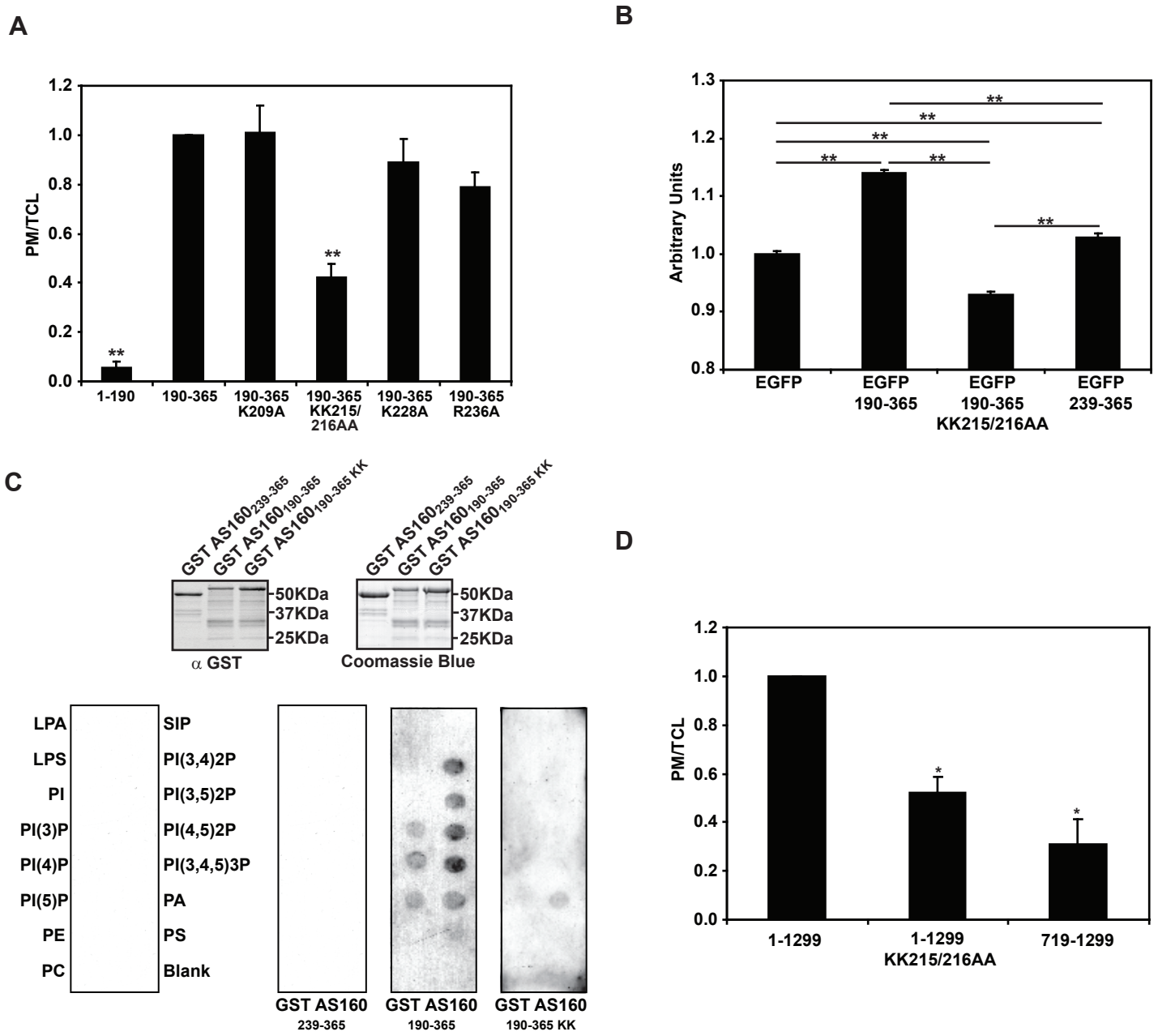
A
PM/TCL
1.2
1.0
0.8
0.6
0.4
0.2
0.0
**
**
1-190
190-365
190-365 K209A
190-365 KK215/ 216AA
190-365 K228A
190-365 R236A
B
Arbitrary Units
1.3
1.2
1.1
1.0
0.9
0.8
**
**
**
**
**
EGFP
EGFP 190-365
EGFP 190-365 KK215/216AA
EGFP 239-365
C
GST AS160239-365
GST AS160190-365
GST AS160190-365 KK
50KDa
37KDa
25KDa
α GST
Coomassie Blue
LPA
LPS
PI
PI(3)P
PI(4)P
PI(5)P
PE
PC
SIP
PI(3,4)2P
PI(3,5)2P
PI(4,5)2P
PI(3,4,5)3P
PA
PS
Blank
GST AS160 239-365
GST AS160 190-365
GST AS160 190-365 KK
D
PM/TCL
1.2
1.0
0.8
0.6
0.4
0.2
0.0
*
*
1-1299
1-1299 KK215/216AA
719-1299

Figure 4:

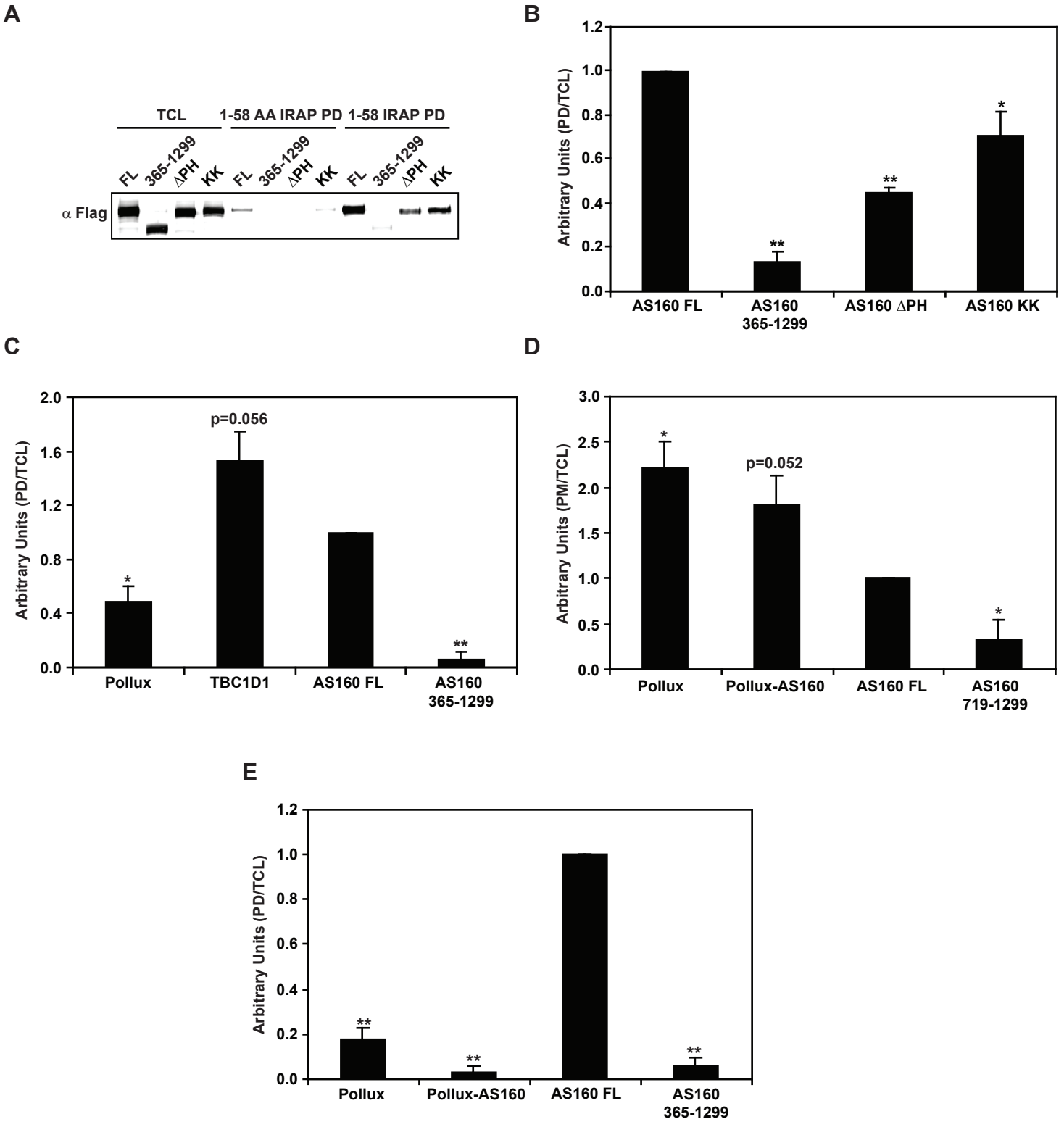
A
TCL
1-58 AA IRAP PD
1-58 IRAP PD
FL
365-1299
ΔPH
KK
α Flag
B
Arbitrary Units (PD/TCL)
AS160 FL
AS160 365-1299
AS160 ΔPH
AS160 KK
C
Arbitrary Units (PD/TCL)
p=0.056
Pollux
TBC1D1
AS160 FL
AS160 365-1299
D
Arbitrary Units (PM/TCL)
p=0.052
Pollux
Pollux-AS160
AS160 FL
AS160 719-1299
E
Arbitrary Units (PD/TCL)
Pollux
Pollux-AS160
AS160 FL
AS160 365-1299

Figure 5:

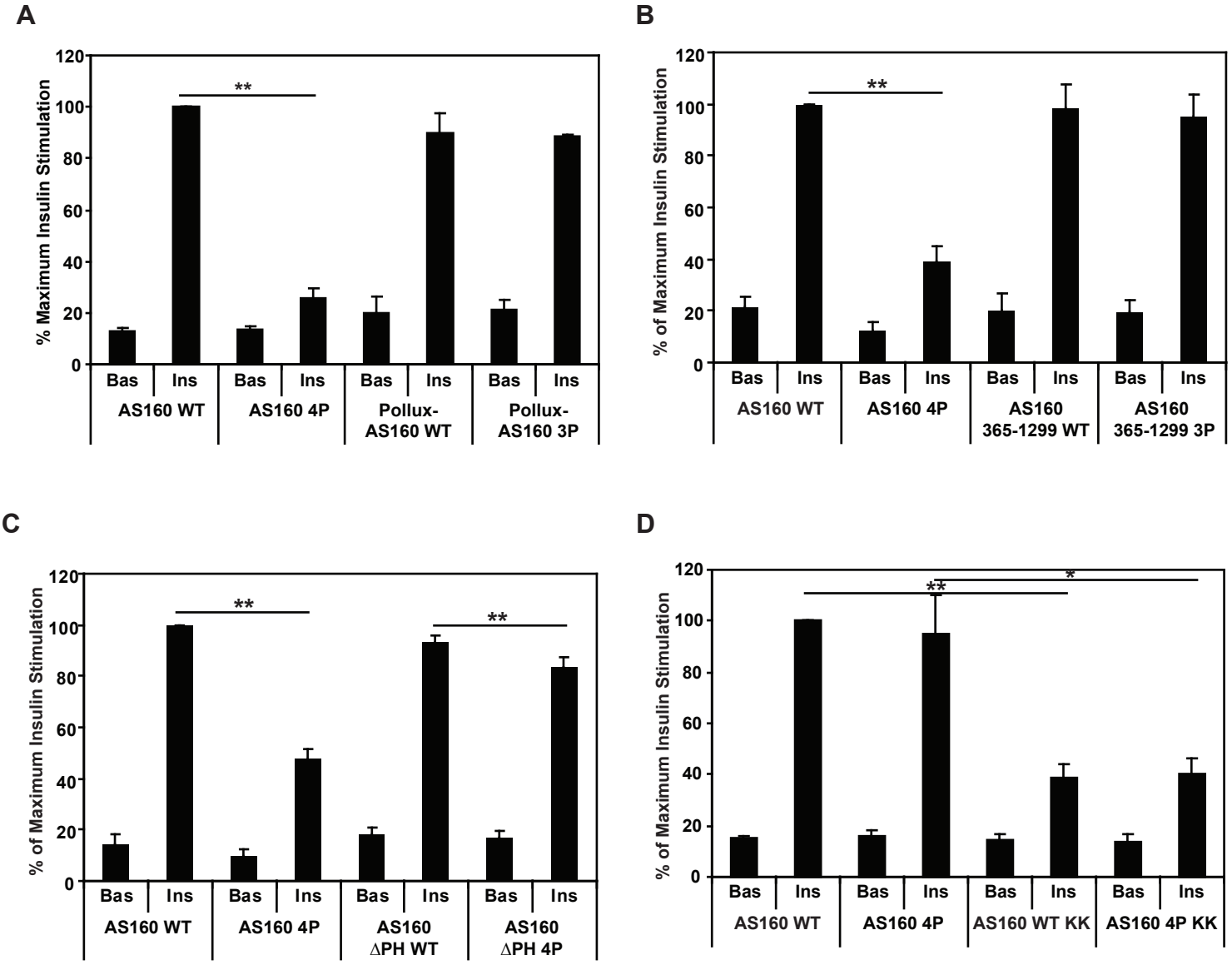
A
% Maximum Insulin Stimulation
120
100
80
60
40
20
0
**
Bas
Ins
AS160 WT
AS160 4P
Pollux-AS160 WT
Pollux-AS160 3P
B
% of Maximum Insulin Stimulation
AS160 WT
AS160 4P
AS160 365-1299 WT
AS160 365-1299 3P
C
% of Maximum Insulin Stimulation
AS160 WT
AS160 4P
AS160 ΔPH WT
AS160 ΔPH 4P
D
% of Maximum Insulin Stimulation
*
AS160 WT
AS160 4P
AS160 WT KK
AS160 4P KK

Figure 6:

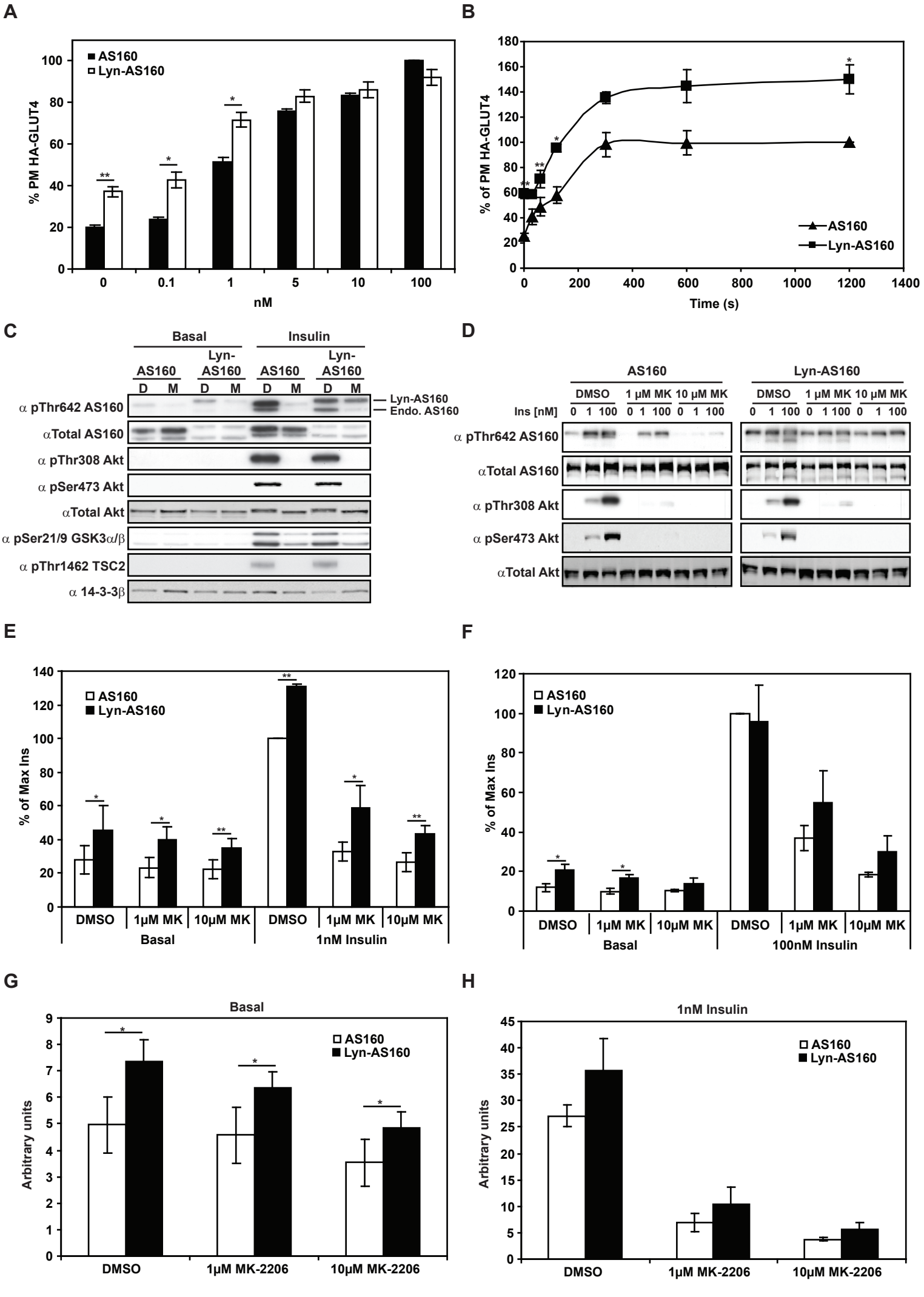
A
AS160
Lyn-AS160
% PM HA-GLUT4
nM
B
% of PM HA-GLUT4
Time (s)
AS160
Lyn-AS160
C
Basal
Insulin
AS160
Lyn-AS160
D M
Lyn-AS160
Endo. AS160
α pThr642 AS160
αTotal AS160
α pThr308 Akt
α pSer473 Akt
αTotal Akt
α pSer21/9 GSK3α/β
α pThr1462 TSC2
α 14-3-3β
D
AS160
Lyn-AS160
DMSO
1 μM MK
10 μM MK
Ins [nM]
E
% of Max Ins
DMSO
1μM MK
10μM MK
Basal
1nM Insulin
F
100nM Insulin
G
Basal
Arbitrary units
DMSO
1μM MK-2206
10μM MK-2206
H
1nM Insulin

Figure 7:

A

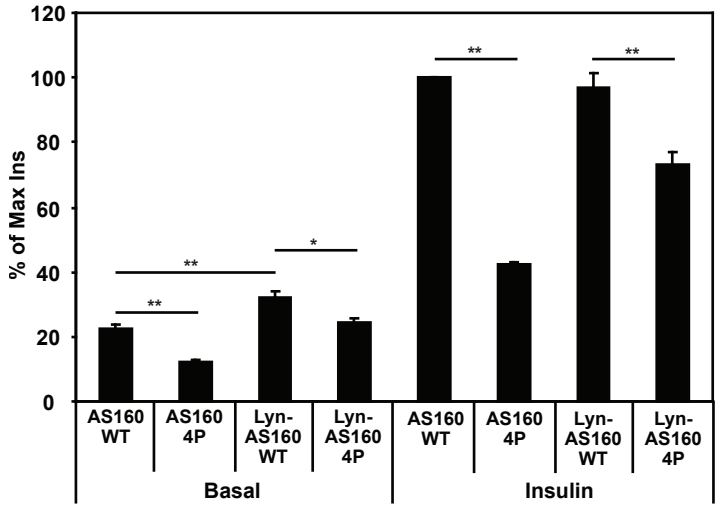
120
100
80
60
40
20
0
% of Max Ins
**
**
*
**
**
AS160 WT
AS160 4P
Lyn-AS160 WT
Lyn-AS160 4P
AS160 WT
AS160 4P
Lyn-AS160 WT
Lyn-AS160 4P
Basal
Insulin

B

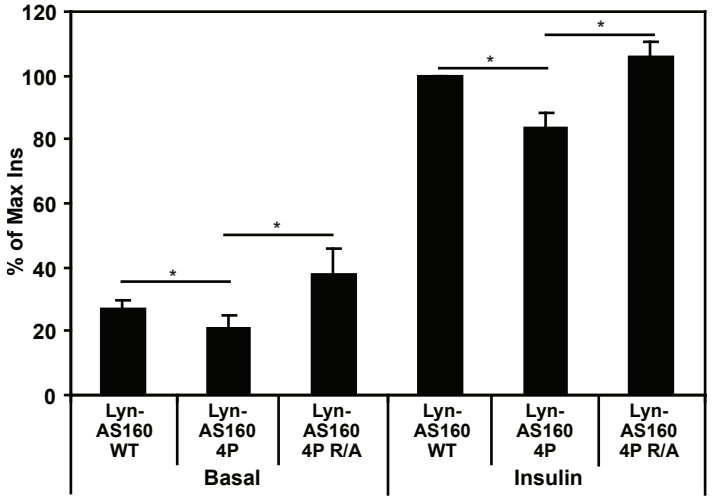
120
100
80
60
40
20
0
% of Max Ins
*
*
*
*
Lyn-AS160 WT
Lyn-AS160 4P
Lyn-AS160 4P R/A
Lyn-AS160 WT
Lyn-AS160 4P
Lyn-AS160 4P R/A
Basal
Insulin

C

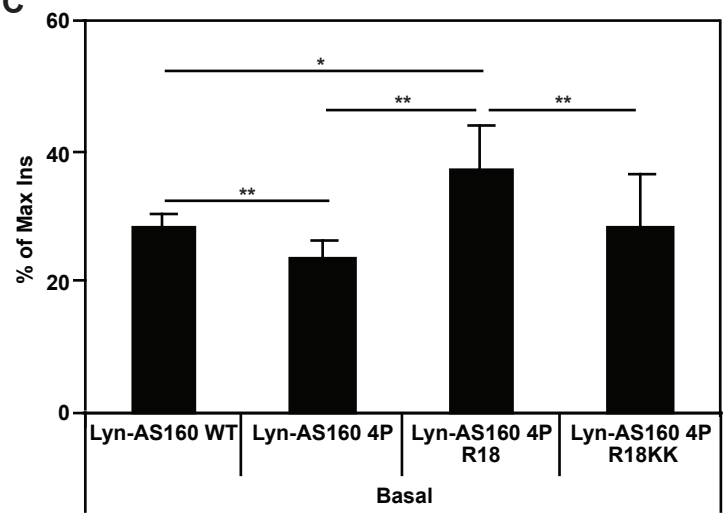
60
40
20
0
% of Max Ins
*
**
**
**
Lyn-AS160 WT
Lyn-AS160 4P
Lyn-AS160 4P R18
Lyn-AS160 4P R18KK
Basal

Supplementary Figure 1:

A

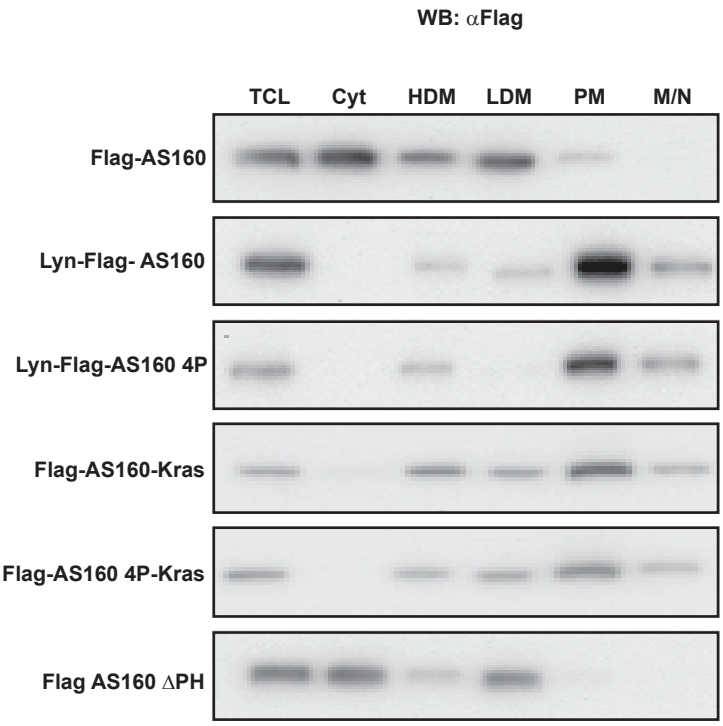

B

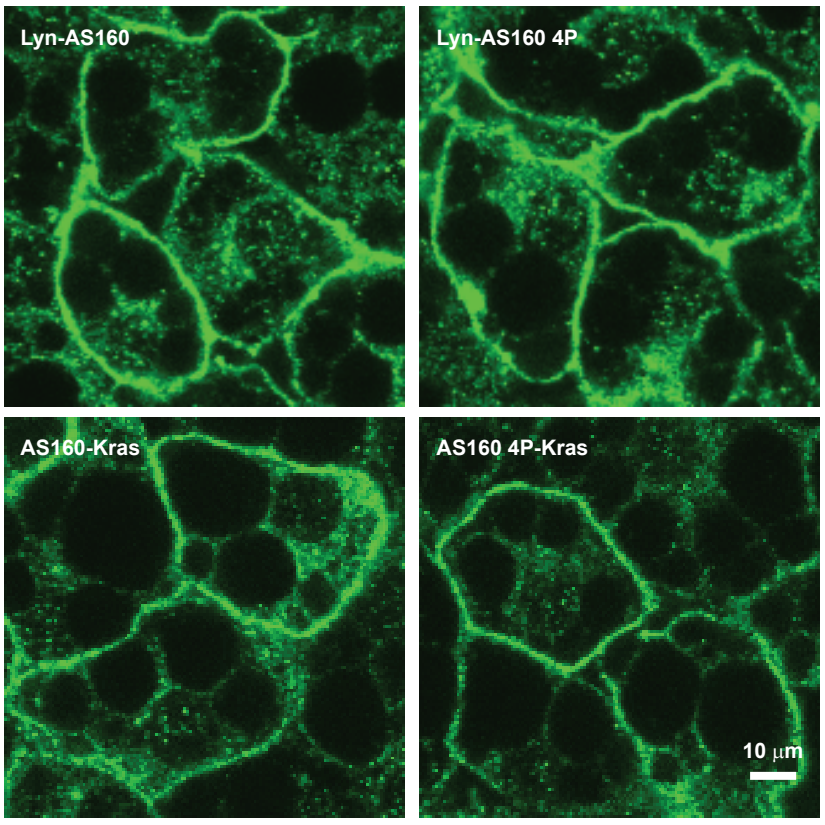

Supplementary Figure 2:

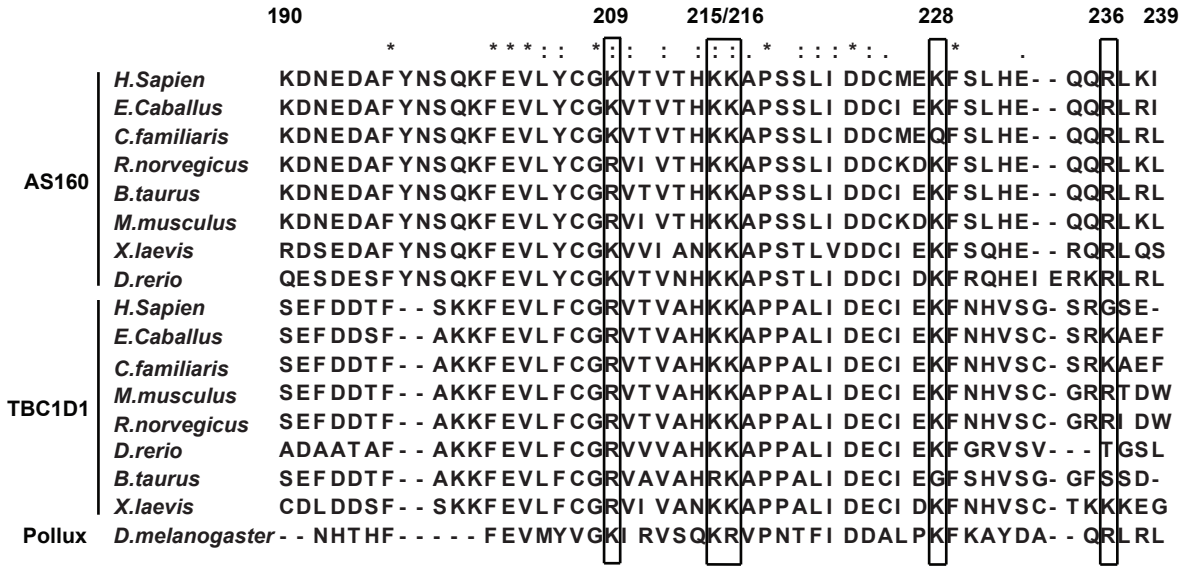

Supplementary Figure 3:

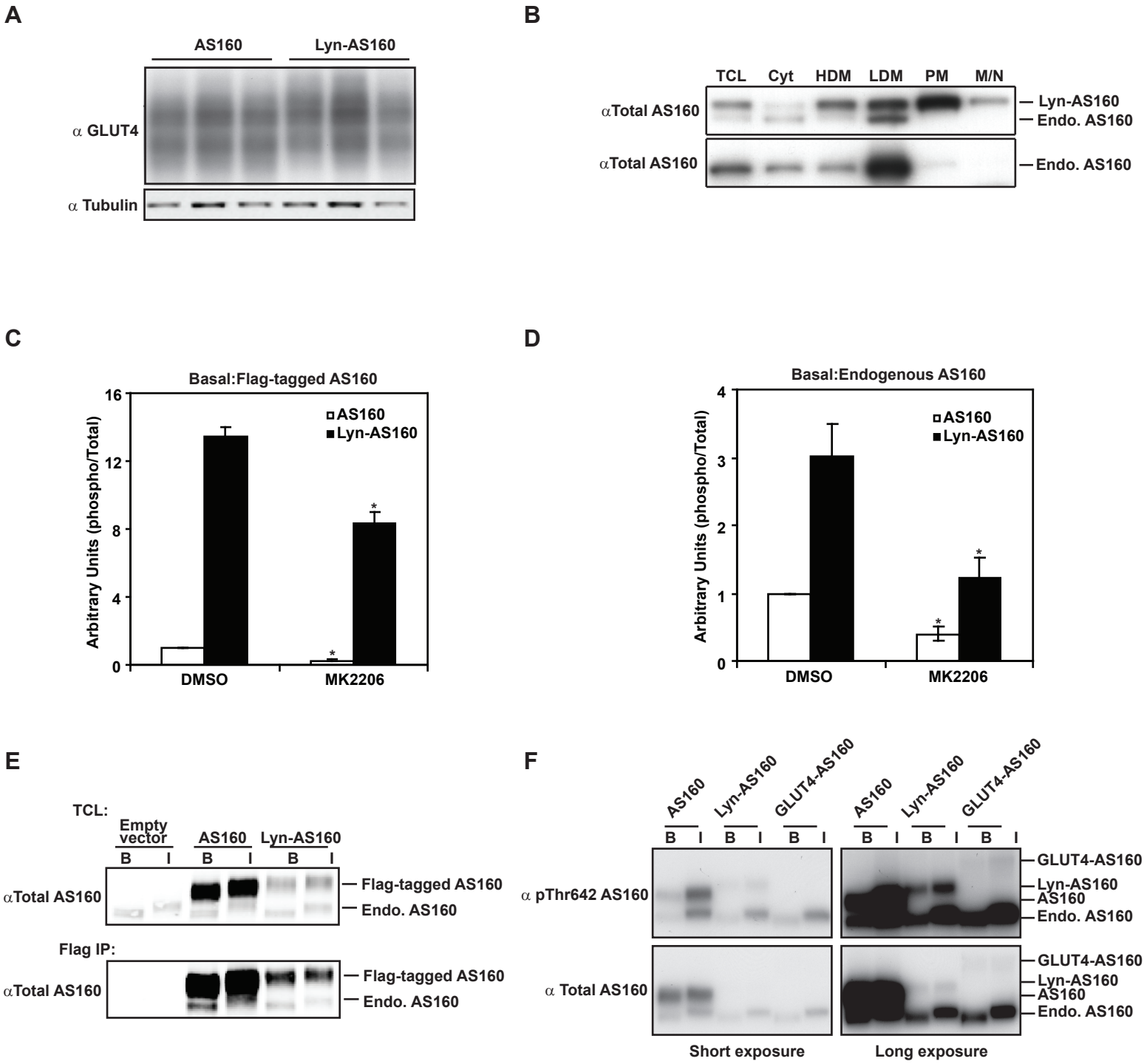

Supplementary Figure 4: